Department of Chemistry
University of Helsinki
Finland

Advanced separation techniques combined with mass spectrometry for difficult analytical tasks – isomer separation and oil analysis

Jaakko Laakia

Academic Dissertation
To be presented, with the permission of
the Faculty of Science of the University of Helsinki,
for public criticism in Auditorium A129 of the Department of Chemistry
(A.I. Virtasen aukio 1, Helsinki)
on May 12th, 2017, at 12 o'clock noon.

Helsinki 2017

Supervisors	Professor Tapio Kotiaho Department of Chemistry Faculty of Science and Division of Pharmaceutical Chemistry and Technology Faculty of Pharmacy University of Helsinki Docent Tiina Kauppila Division of Pharmaceutical Chemistry and Technology Faculty of Pharmacy University of Helsinki
Reviewers	Professor Janne Jänis Department of Chemistry Faculty Science and Forestry University of Eastern Finland Docent Velimatti Ollilainen Department of Food and Environmental Sciences Faculty of Agriculture and Forestry University of Helsinki
Opponent	Professor Wolfgang Schrader Max-Planck-Institut für Kohlenforschung Mülheim an der Ruhr, Germany
Custos	Professor Marja-Liisa Riekkola Department of Chemistry University of Helsinki

ISBN 978-952-336-016-7 (Paperback)
ISSN 0782-6117
Erweko Oy
Helsinki 2017

ISBN 978-952-336-017-4 (PDF)
http://ethesis.helsinki.fi
Helsingin yliopiston verkkojulkaisut

TABLE OF CONTENTS

FINNISH METEOROLOGICAL INSTITUTE

		Series title, number and report code of publication
Published by	Finnish Meteorological Institute (Erik Palménin aukio 1) , P.O. Box 503 FIN-00101 Helsinki, Finland	Finnish Meteorological Institute Contribution 131, FMI-CONT-131 Date May 2017

Author:
Jaakko Laakia

Title:
Advanced separation techniques combined with mass spectrometry for difficult analytical tasks – isomer separation and oil analysis

Abstract

This thesis covers two aspects of utilisation of advanced separation technology together with mass spectrometry: 1. Drift tube ion mobility spectrometry – mass spectrometry (IMS-MS) studies of the behaviour of ions in the gas phase and 2. Comprehensive two dimensional gas chromatography – time-of-flight mass spectrometry (GC×GC-TOF-MS) studies for characterization of crude oil samples.

In IMS studies, the focus was on the separation of isomeric compounds. For example, [M-H]- ions of 2,4-di-tert-butylphenol (2,4-DtBPh) and 2,6-di-tert-butylphenol (2,6-DtBPh) were separated. It was also observed that shielding of the charge site by the functional groups of a molecule has a large effect on the separation of the isomeric compounds. For example, amines with a shielded charge site were separated from those with a more open charge site, while some of the isomeric amines studied were not separated. Different kinds of adduct ions were observed for some of the analytes. Dioxygen adducts were seen for 2,4-DtBPh [M+O2]-, 2,6-di-tert-butylpyridine (2,6-DtBPyr) [M+O2]+· and 2,6-di-tert-butyl-4-methylpyridine (2,6-DtB-4MPyr) [M+O2]+·. The adduct formation increases the total mass of the analyte ion, and therefore, for example the 2,4-DtBPh [M+O2]- ion could be separated from its isomeric compound 2,6-DtBPh [M-H]-, which did not from the dioxygen adduct ion. In the case of 2,6-DtBPyr and 2,6-DtB-4MPyr, the [M]+ ions formed dioxygen adduct [M+O2]+· ions. The both ions, [M]+ and [M+O2]+·, shared the same drift time which was longer than their [M+H]+ ion species. This work demonstrates that measuring with IMS the mobility of different ion structures of the same molecule, especially dioxygen adducts, results in a better understanding of the role of adduct ions in the IMS-separation process.

In GC×GC-TOF-MS studies, the focus was on detailed characterization of crude oil samples. For instance, oils from the Recôncavo Basin were classified to two different groups by using minor oil components. The GC×GC-TOF-MS data showed the correlation between 2D retention time and the number of carbons in a ring for several hydrocarbons as known from the literature. This information was used to achieve more structural information about eight new tetracyclic compounds, some of them similar to nor-steranes, detected during analysis. Some of these new compounds could be used as maturity indicators. This study demonstrated how GC×GC-TOF-MS can be used to separate geochemically interested isomers, identify minor geochemical differences between oils and achieve structural information about unknown biomarkers.

Publishing units
Atmospheric Composition Research and Expert Services

Classification (UDC)			Keywords
543.544.3	543.51	539.144.7	Ion mobility spectrometry, Two-dimensional gas chromatography, mass spectrometry, oil analysis, isomer separation

ISSN and series title
0782-6117 Finnish Meteorological Institute Contributions

ISBN	Language	Pages
978-952-336-016-7 (Paperback) 978-952-336-017-4 (PDF)	English	121

ILMATIETEEN LAITOS

Julkaisun sarja, numero ja raporttikoodi
Finnish Meteorological Institute
Contribution 131, FMI-CONT-131

Julkaisija Ilmatieteen laitos, (Erik Palménin aukio 1)
PL 503, 00101 Helsinki

Julkaisuaika: Toukokuu 2017

Tekijä:
Jaakko Laakia

Nimeke
Massaspektometriin kytketyt kehittyneet esierotustekniikat vaikeissa analyyttisissa tehtävissä – isomeerien erotuksessa ja öljyanalytiikassa

Tiivistelmä

Väitöskirja koostuu kahdesta osiosta. Ensimmäisessä osiossa perehdytään ioniliikkuvuusspektrometria–massaspektrometriaan (IMS-MS), jolla tutkittiin ionien liikkuvuutta kaasufaasissa, ja toisessa kaksiulotteiseen kaasukromatografia–massaspektrometriaan (GC×GC-TOF-MS), jolla karakterisoitiin raakaöljynäytteitä.
Yksi IMS tutkimuksen tavoitteista oli erotella isomeerejä. Osa tutkituista isomeereistä erottui hyvin ja osa ei. Tarkemmassa tarkastelussa huomattiin, että yhdisteiden tietyt funktionaaliset ryhmät pystyvät ”suojaamaan” molekyylin varautunutta funktionaalista ryhmää. Tällä efektillä oli suuri merkitys isomeerien erottumisessa, sillä esimerkiksi amiinit, joiden varauskohta oli ”suojattu” erottuivat IMS:llä ioneista, joiden varauskohta oli ”avoimempi”. Erilaisia addukti-ioneja (analyytin ja pienmolekyylin yhteenliittymä) havaittiin joillekin mitatuille yhdisteille. Mikäli adduktin muodostus tapahtuu vain toiselle isomeerille niin isomeerit erottuvat IMS:lla esim. 2,4-di-tert-butylphenolien (2,4-DtBPh) muodosti [M+O2]-· addukti-ionin ja erottui 2,6-DtBPh-isomeeristä mikä ei muodostanut vastaavaa addukti-ionia. di-tert-butyilipyridiini taas muodosti [M]+ ja [M+O2]+·ionin. Näille molemmille ioneille mitattiin sama liikkuvuus, mutta se pystyttiin erottamaan saman yhdisteen eri ioni muodosta, [M+H]+, IMS:llä. Tutkimuksessa osoitettiin, että on tärkeää mitata liikkuvuus saman yhdisteen eri ionimuodoille, erityisesti dihappiaddukteille, jotta ymmärrettäisiin paremmin ionien muodomismekanismeja sekä adduktien vaikutusta eri ionimuotojen ja isomeerien erottumiselle IMS:ssä.
Väitöskirjan GC×GC-TOF-MS osiossa karakterisoitiin raakaöljynäytteitä. Esimerkiksi Brasilian Recôncavo Basin öljykentältä kerätyt näytteet voitiin jakaa kahteen ryhmään käyttämällä näytteiden luokitukseen alhaisen pitoisuuden näytekomponentteja. GC×GC-TOF-MS mittaukset osoittivat korrelaation toisen dimensio GC-erotuksen retentioajan ja tunnettujen saturoituneiden hiilivetyjen renkaiden määrän ja niissä olevien hiiliatomien lukumäärän välillä. Tätä tietoa käytettiin hyödyksi tutkittaessa kahdeksan tuntemattoman yhdisteen rakennetta, joista osalla oli samankaltainen rakenne kuin nor-steraaneilla. Kahta näistä yhdisteistä voitiin hyödyntää öljyjen maturaatiotasojen määrityksessä. Tutkimuksessa näytettiin että GC×GC-TOF-MS:llä voidaan erotella toisistaan geokemiallisesti kiinnostavia isomeerejä, tunnistaa pieniä geokemiallisia eroja öljyjen välillä ja saada rakenteellista tietoa ennestään tuntemattomista biomarkkereista.

Julkaisijayksikkö
Ilmakehän koostumuksen tutkimus ja asiantuntijapalvelut

Luokitus (UDK)
543.544.3 543.51 539.144.7

Asiasanat
Ioniliikkuvuusspektrometria, kaksiulotteinen kaasukromatografia, massaspektrometria, isomeerien erottelu, öljytutkimus

ISSN ja avainnimike
0782-6117 Finnish Meteorological Institute Contributions

ISBN
978-952-336-016-7 (Nidottu)
978-952-336-017-4 (PDF)

Kieli Englanti

Sivumäärä 121

LIST OF ORIGINAL PAPERS

This thesis is based on the following papers, hereafter referred to by their Roman numerals [**I-V**]:

I J. Laakia, C. S. Pedersen, A. Adamov, J. Viidanoja, A. Sysoev, T. Kotiaho, Sterically Hindered Phenols in Negative Ion Mobility Spectrometry-Mass Spectrometry. Rapid Comm. Mass Spectrom. 2009, 23, 3069-3076

II J. Laakia, A. Adamov, M. Jussila, C. S. Pedersen, A. Sysoev, T. Kotiaho, Separation of Different Ion Structures in Atmospheric Pressure Photoionization - Ion Mobility Spectrometry - Mass Spectrometry (APPI-IMS-MS). J. Am. Soc. Mass Spectrom. 2010, 21, 1565-1572

III J. Laakia, T. J. Kauppila, A. Adamov, A. A. Sysoev, T. Kotiaho, Separation of isomeric amines with ion mobility spectrometry (IMS), Short communication, Talanta. 2015, 135, 889-893

IV A. Casilli, R. C. Silva, J. Laakia, C. J. F. Oliveira, A. A. Ferreira, M. R. Loureiro, D. A. Azevedo, F. R. Aquino Neto, High resolution molecular organic geochemistry assessment of Brazilian lacustrine crude oils, Org. GeoChem. 2014, 68, 61-70

V J. Laakia, A. Casilli, Bruno Q. Araújo, F. T. T. Gonçalves, E. Marotta, C. J. F. Oliveira, C. A. Carbonezi, M. R. B. Loureiro, D. A. Azevedo, F. R. Aquino Neto, Characterization of unusual tetracyclic compounds and possible novel maturity parameters for Brazilian crude oils using Comprehensive Two-Dimensional Gas Chromatography - Time of Flight Mass Spectrometry, Org. GeoChem. Accepted for publication 2016. (http://dx.doi.org/10.1016/j.orggeochem.2016.10.012)

Author´s contribution to the publications included in the doctoral thesis:

Papers I-III. Main responsibility in planning and carrying out measurements, data processing and writing the article. Associate professor Alexey Sysoev has used his contribution (consulting in physics of IMS and IMS/MS) in Papers I and II in his Doctor of Science degree at the National Research Nuclear University MEPhI, Moscow, Russia.

Paper IV Main responsibility in data processing and shared responsibility in geochemical analysis and in writing of the article, excluding the maturation (diamondoids) results, which were carried out by Renzo C. Silva and used as part of his PhD thesis "Applications of modern analytical techniques in petroleum organic geochemistry studies" at Federal University of Rio de Janeiro, Rio de Janeiro, Brazil.

Paper V Main responsibility in data processing and in geochemical analysis and in writing of the article.

ACKNOWLEDGEMENTS

This thesis is based on research conducted by the Ion Mobility Group of the Laboratory of the Analytical Chemistry at the University of Helsinki and the Laboratory of the Molecular Organic Geochemistry and Environmental at the Federal University of Rio de Janeiro, Brazil. The Academy of Finland (project numbers: 114132 and 122018), is acknowledged for financial support for the ion mobility research during the years 2007-2010 and PETROBRAS (Contract 00500072201.11.9) for funding the geochemistry research during the years 2012-2014. The Brazilian organizations CNPq, FAPERJ and FUJB are thanked for their financial support. Water och Lisi Wahls stiftelse för naturevetenskaplig forsking is thanked for funding a new nitrogen generator.

All of the staff (especially Pena) of the Laboratory of Analytical Chemistry and of the Laboratory of the Molecular Organic Geochemistry and Environmental (especially Vinicius) are acknowledged for providing assistance and the facilities.

I would like to thank all of the ion mobility team members: Ph.D. Alexey Adamov and Prof. Alexey Sysoev for their technical assistance, Ph.D. Christian Pedersen for supportive and innovative comments and Dos. Tiina Kauppila and Prof. Tapio Kotiaho for supervising my work and the geochemistry team: Prof. Débora Azevedo, Ph.D. Alessandro Casilli and Prof. Francisco R. Aquino Neto for constructive comments, Prof. Maria Regina Loureiro is especially thanked for her great help in Geochemistry, Portuguese and English.

Acknowledgements are also directed to helpful colleagues: Ph.D. Jaroslaw Puton, Ph.D. Anna-Kaisa Viitanen, Ph.D. Elina Kalenius, Ph.Lic. Matti Jussila, Ph.D. Timo Mauriala, Ph.D. Markus Haapala, Ph.Lic. Jyrki Viidanoja, Ph.D. Renzo C. Silva, M.Sc. Cleverson J.F. Oliveira and Ph.D. Alexandre A. Ferreira.

ABBREVIATIONS

^{1}D	First chromatographic dimension
^{2}D	Second chromatographic dimension
ACN	Acetonitrile
APCI	Atmospheric pressure chemical ionization
APPI	Atmospheric pressure photoionization
B/C	Branched and cyclic hydrocarbon fraction
B-N	Bradbury-Nielsen gate
2-*t*BPh	2-*tert*-Butylphenol
2-*t*BPyr	2-*tert*-Butylpyridine
β-car	β-Carotane
DBE	Double bond equivalence
CENPES	The Research Center of Petrobras (Centro de Pesquisas Leopoldo Américo Miguez de Mello, Rio de Janeiro, RJ, Brazil)
2,4,6-Col	2,4,6-Collidine
CV	Compensation voltage
2,6-D*t*B-4-MPh	2,6-Di-*tert*-butyl-4-methylphenol
2,4-D*t*BPh	2,4-Di-*tert*-butylphenol
2,6-D*t*BPh	2,6-Di-*tert*-butylphenol
2,6-D*t*B-4-MPyr	2,6-Di-*tert*-butyl-4-methylpyridine
2,6-D*t*BPyr	2,6-Di-*tert*-butylpyridine
DH_{30} (or $DiaH_{30}$)	C_{30} 17α-Diahopane
N,*N*-DMA	*N*,*N*-Dimethylaniline
DMS	Differential mobility spectrometry (= also FAIMS)
EI	Electron ionization
ESI	Electrospray ionization
4-EA	4-Ethylaniline
FAIMS	Field asymmetric waveform ion mobility spectrometry (= also DMS)
FID	Flame ionization detector
Gam	Gammacerane
GC	Gas chromatography
GC×GC	Two-dimensional gas chromatography
GC×GC-TOF-MS	Two-dimensional gas chromatography – time-of-flight mass spectrometry
H_{30}	17α(H),21β(H)-Hopane
$H_{31}R$	C_{31} 17α(H),21β(H)-homohopane
IMS	Ion mobility spectrometry
IMS-FP	Ion mobility spectrometer – faraday plate detector
IMS-MS	Ion mobility spectrometer – mass spectrometer
LC	Liquid chromatography
m/z	Mass to charge ratio
M_{30}	Moretane, 17β(H),21β(H)-hopane
$3\beta MH_{31}$	C_{31} 3β-Methylhopane
MeOH	Methanol
n-M-*o*-T	*N*-Methyl-*o*-toluidine

x-MBA	x-Methylbenzylamine (x = 2, 3, or 4)
ONII	8α(H), 14α(H)-Onocerane
ONIII	8α(H), 14β(H)-Onocerane
PEA	2-Phenethylamine
R_o(%)	Vitrinite reflectance
RF	Radio-frequency
RIP	Reaction ion peak
SIM	Selected ion monitoring
St	20*S* + 20*R* C_{27} 5α,14α,17α-Cholestanes
TeT_{24}	C_{24} Tetracyclic terpane
Tm	C_{27} 17α-22,29,30-Trisnorhopane
t_R	Retention time
TIMS	Trapped ion mobility Spectrometer
Tr_x	C_x tricyclic terpane
Ts	C_{27} 18α-22,29,30-Trisnorneohopano
TOF-MS	Time-of-flight mass spectrometry
TWIMS	Traveling wave ion mobility spectrometry
2,4,6-T*t*BPh	2,4,6-Tri-*tert*-butylphenol
2,4,6-TNT	2,4,6-Trinitrotoluene

1. INTRODUCTION

Mass spectrometry (MS) is a powerful analytical technique, which is used for the identification of unknown compounds and for the quantitation of known compounds in various types of samples [1]. It is used in many fields of science for these purposes, for example in pharmaceutical chemistry, environmental and food analysis, forensic science and industrial process analysis. The working principle of MS involves first the ionization of the compounds to be measured and the subsequent separation of the ions based on their differing mass-to-charge (*m/z*) ratios. Ionization can be carried out in atmospheric pressure or in a vacuum, but ion separation is always done in a vacuum. Production of *m/z* data is the key feature of MS, since it allows the determination of the molecular weight of a compound. The current mass spectrometers can measure very precisely the *m/z* ratios, which allows the determination of elemental composition of the analytes. However, the elemental composition of a compound does not necessarily give information about the chemical structure, since compounds can have the same elemental compositions, but different structures (isomeric compounds). One solution for this is the separation of isomeric compounds before the mass spectrometric analysis. In addition, mass spectrometric analysis of very complex samples, such as biological or crude oil samples, often requires additional pre-separation of the sample components for reliable analysis.

The two most common pre-separation techniques used with MS are liquid chromatography (LC) [2] and gas chromatography (GC) [3]. However, they are not always sufficient for reliable compound identification, for example in complex samples containing isomeric compounds, which are not separated (co-elutes) in LC or GC. Therefore, alternative and advanced pre-separation techniques, such as ion mobility spectrometry (IMS) [4] and two dimensional gas chromatography (GC×GC) [5], that can be combined with MS, have been developed. Their analytical characteristics are studied in this thesis.

Similar to MS, in IMS the compounds are first ionized and subsequently separated. However, in IMS the ion separation typically occurs in the gas phase under atmospheric pressure or in a reduced pressure, which is higher than in MS. The other main difference is that in IMS the ions are separated based on their shape (i.e. collision cross-section)

[4] instead of *m/z* ratios as in MS. In many cases IMS is more capable to separate isomers than MS.

In GC×GC the main idea is to use two different column phases in line, for example, a non-polar column in the first dimension (^{1}D) and a semi-polar column in the second dimension (^{2}D). This results in GC×GC providing clearly higher peak capacity than one dimensional GC, and very complex samples, such as crude oil samples containing thousands of compounds, can be more efficiently separated into individual compounds [5-9]. This makes GC×GC-MS analysis more reliable than GC-MS analysis.

1.1.1 Basic operation principles of ion mobility spectrometry

The operation principle and main parts of the most common IMS, the drift tube, is presented in Figure 1. A drift tube IMS consists of an ion source, a desolvation region, a drift region, a detector, control electronics and software to run the instrument.

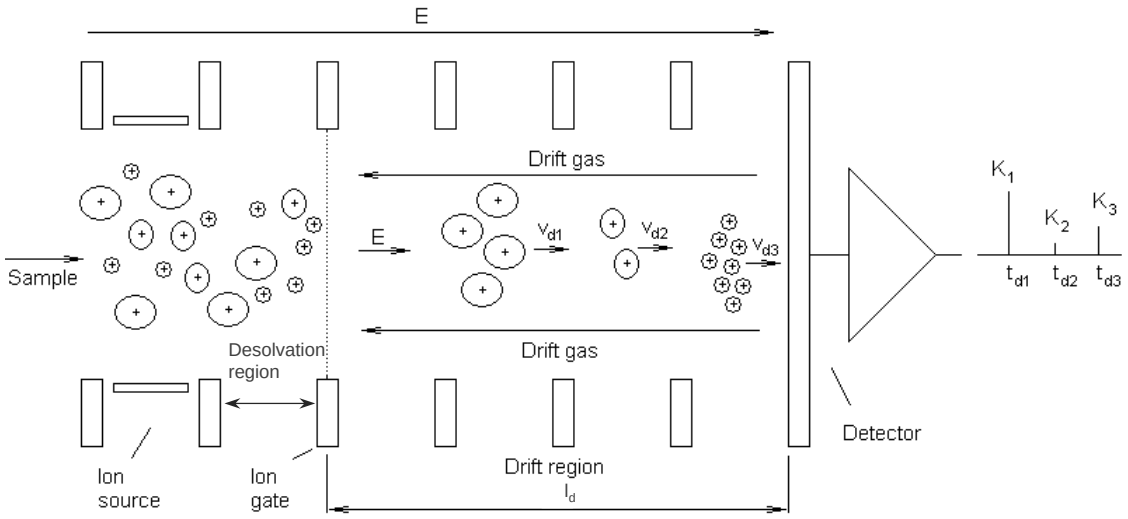

Figure 1. Schematic diagram of a drift tube IMS (permission and courtesy of Alexey Sysoev, unpublished material). l_d = length of the drift region, E = electric field, v_{dx} = drift velocity of an ion, K_x = mobility coefficient of an ion and t_{dx} = drift time of an ion.

A typical measurement sequence has the following steps: After sample introduction the analyte molecules are ionized in an atmospheric pressure ion source and the ions are transferred to the desolvation area, where the ions are stored before they are pulsed with a Bradbury-Nielsen (B-N) gate [11] into the drift region. Next, the ions move by an electric field (typically 100-300 V/cm) across the drift region, in which a neutral gas

(e.g. nitrogen or air) is flowing in the opposite direction. After the IMS separation, the separated ions are usually detected with a faraday plate detector or with MS.

The separation of ions is based on their collisions with neutral gas molecules, which produce different drift times for ions with differing shapes, i.e. differing collision cross-sections (cm^2 or Å). For example, an ion with a small collision cross-section moves faster through the drift region than an ion with a larger collision cross-section. The drift velocity (v_d, [cm/s]) of an ion through the drift region can be presented by Equations 1 and 2 [4, 10].

$$v_d = KE \tag{1}$$

$$v_d = \left(\frac{l_d}{t_d}\right) \Rightarrow K = \left(\frac{l_d^2}{t_d V}\right) \tag{2}$$

where K = mobility coefficient ($cm^2V^{-1}s^{-1}$), E = electric field in the drift region (V/cm), l_d = length of the drift region (cm), t_d = drift time of the ion through the drift region (ms) and V = voltage drop over the drift region (V).

The mobility coefficient (K) (Equation 2) is inversely proportional to collision cross-section (Ω) [10] (Equation 3).

$$K = \frac{3ez\sqrt{2\pi}(1+\alpha_c)}{16N\sqrt{\mu k T_{eff}}\Omega} \tag{3}$$

Where e = charge of electron (C), z = charge number, α_c = correction factor for large molecules <0.02, N = drift gas density (molecules m^{-3}), μ = reduced mass ion-neutral pair (g), k = Boltzmann's constant (J/K), T_{eff} = effective temperature of ion (K).

K is often presented as reduced mobility coefficient K_0 according to Equation 4 [4]:

$$K_0 = \left(\frac{l_d^2}{t_d V}\right)\left(\frac{273}{T}\right)\left(\frac{P}{760}\right) \tag{4}$$

where, T = temperature (K) and P = pressure (Torr).

Even though mobilities in IMS are typically reported as reduced mobility (K_0) values (Equation 4), which are normalized with standard pressure and temperature, variations in reduced mobility values are observed. This can be due to moisture or other impurities in the drift gas, or instrumental factors, such as an imperfect electric field or variation of the drift length. Due to these facts different compounds have been tested as reference compounds, which would allow standardization of mobilities. It has been observed that mobilities of compounds such as tetraalkylammonium halides [11] and 2,6-di-*tert*-butylpyridine [12-14], are not much affected by moisture or other drift gas impurities. Therefore, these compounds can be used for comparison of different instruments as instrumental standards [15]. On the other hand, model compounds such as lutidine [16] and dimethyl methylphosphonate [12], which also respond to the quality (e.g. impurities) changes of the drift gas, can be used as mobility standards. All the above-mentioned compounds are used as standards in positive ion mode measurements. Standard compounds, such as methyl salicylate [17] and 2,4,6-trinitrotoluene [18], to be used as mobility standards in negative ion mode, have also been presented.

Ionization is the heart of an ion mobility spectrometer. Ions are generated in drift tube IMS commonly with a radioactive source (e.g. ^{63}Ni) [19], electrospray ionization (ESI) [4, 11, 20-23], atmospheric pressure chemical ionization (APCI) [24, 25] or atmospheric pressure photoionization (APPI) [26-28]. All these techniques work under atmospheric pressure conditions, and can be considered as soft ionization techniques, which produce mostly protonated and deprotonated molecules with little fragmentation. Since APCI and APPI were used in this study, they are presented in more detail.

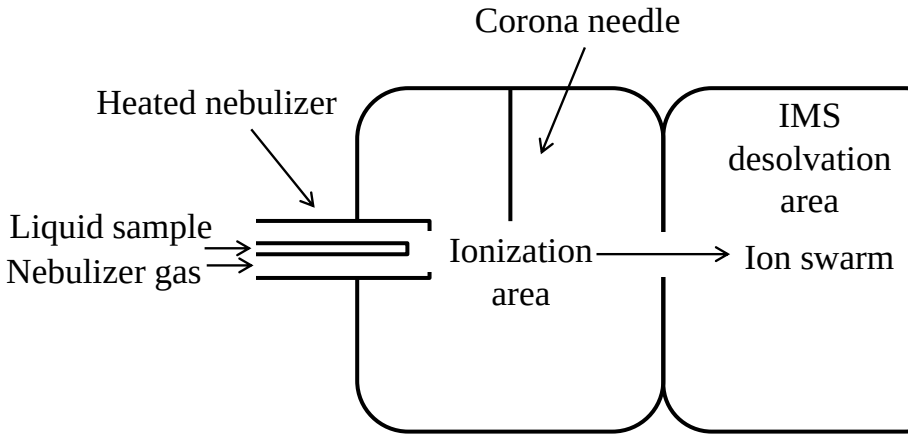

Figure 2. A schematic drawing of a typical atmospheric pressure chemical ionization source for IMS.

As shown in Figure 2, in a typical APCI ion source a liquid sample is pumped through a heated nebulizer, in which a vaporized sample stream is produced with the aid of heat and nebulizer gas [29]. Ionization reactions in APCI are initiated by corona discharge, which is obtained by conducting high voltage to a corona needle. The reactant ions in APCI depend on the solvent composition and reaction ions available in the ionization chamber, and components such as $[H_3O]^+$ and $[NH_4]^+$ ions are formed in positive ion mode, and $[HO]^-$, $[O_3]^-$ and $[NO_x]^-$ ions in negative ion mode [30-34]. In IMS, the reactant ions settle to equilibrium in the desolvation area and typically, a cluster of ions, also called a reactant ion peak (RIP), is observed [4]. The most common analyte ions formed in the ionization reactions with the reactant ions and neutral analyte molecules in APCI are protonated molecules $[M+H]^+$ in positive ion mode and deprotonated molecules $[M-H]^-$ in negative ion mode [4].

APPI ion source resembles the APCI ion source, except that in APPI an ultraviolet (UV) lamp is used to initiate the ionization instead of a corona needle. Often, APPI uses a dopant, an additional solvent, which is introduced to the ion source, in order to enhance the ionization of analytes. In APPI, the ionization sequence typically starts with the ionization of the vaporized solvent or dopant due to radiation emitted by the UV lamp. Various types of reactant ions can be formed in positive APPI, e.g., protonated molecules $[S+H]^+$ or radical cations $[S]^{+\cdot}$ of solvent and / or dopant [35]. In negative APPI, deprotonated molecules $[S-H]^-$ or negative molecular ions $[S]^{-\cdot}$ of solvent and/or atmospheric gases are typically formed [36, 37]. Subsequent reactions of analytes with the reactant ions produce analyte ions; in positive APPI mainly radical cations $M^{+\cdot}$ and/or protonated molecules $[M+H]^+$, and in negative APPI negative molecular ions $M^{-\cdot}$ and/or deprotonated molecules $[M-H]^-$.

The drift tube ion mobility instrument presented above is the main type of IMS instrument used nowadays, but many other types of instruments have been developed and are also commercially available. One of them is field asymmetric waveform ion mobility spectrometry (FAIMS) or differential mobility spectrometry (DMS). The ion separation principle for FAIMS and DMS is the same [38], but the electrode in FAIMS has cylindrical geometry and in DMS planar geometry. The electric field can be varied quickly between high (~20 kV/cm) and low field (~1 kV/cm) using high radio-frequency (RF) voltage also called dispersion or direct voltage (DV) (Figure 3) [39]. An additional superimposed direct current (DC) voltage, a so-called compensation voltage

(CV) is used to allow the passage of the desired ions through the electrode pair to the detector. Scanning the CV creates an analyte spectrum [40].

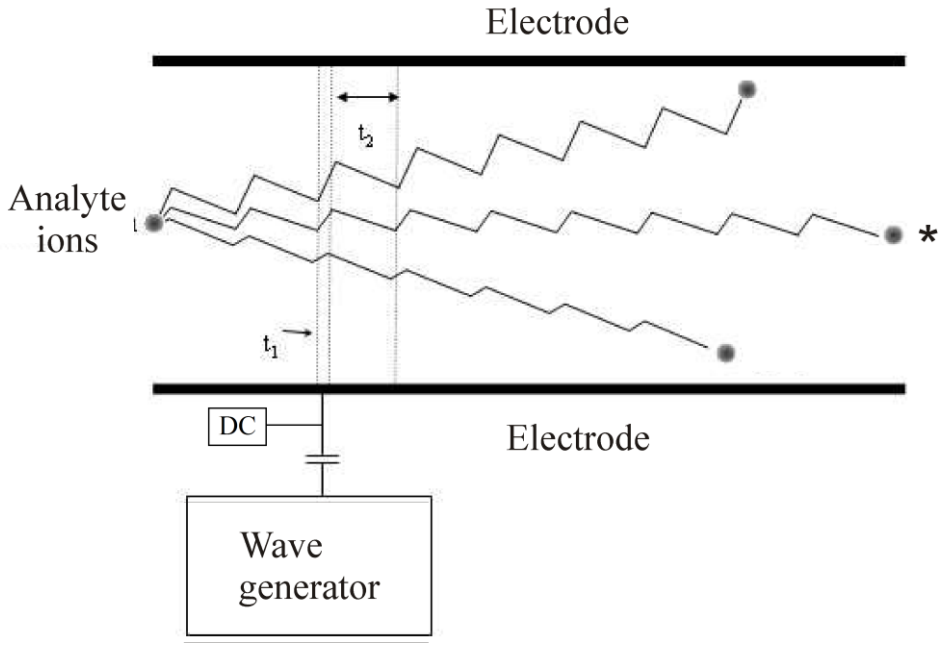

Figure 3. The schematic picture of a field asymmetric waveform ion mobility spectrometry (FAIMS) or differential mobility spectrometry (DMS) represents the situation where the ion (marked with an asterisk) is collected onto the detector. Commonly, the drift gas flow is parallel to the analyte movement (from left to right). t_1 = dispersion voltage (DV) at high field, t_2 = DV at low field and DC = direct current (Reused with permission from ref. [4])

Another IMS approach, which has been combined with mass spectrometry is travelling wave ion mobility spectrometry (TWIMS, Waters Corp., Milford, MA, USA) [41, 42]. In TWIMS a low electric field is used to produce voltage waves (~20 V), which travel through a set of electrodes forming the drift region. Analyte ions are separated as the wave travels through the drift region under reduced pressure (~1 mbar), which is higher than the typical pressure inside a mass analyzer ($<10^{-5}$ mbar).

Recently a trapped ion mobility spectrometer (TIMS)-q-TOF instrument has been developed. In TIMS analyte ions are held stationary in the gas flow [43].

All the presented IMS instrument types have been combined with MS, (IMS-MS [4, 20, 44]) or LC and MS (e.g. LC-FAIMS-MS [45] and LC-IMS-MS [46]). For instance, in biomolecule analysis, where samples are very complex, the IMS-MS combination has increased the component separation [47, 48] and a further increase is obtained with LC-IMS-MS, as thousands of peaks have been separated with different retention times, drift times and *m/z* ratios from plasma proteome [49].

1.1.2 Applications of ion mobility spectrometry

The most important applications of traditional stand-alone IMS instruments are detection of explosives and chemical weapons [50-52]. Besides these, IMS is nowadays used in many fields of science [53, 54]. Ion mobility instruments are typically operated at atmospheric pressure, and therefore do not require heavy vacuum pumps as MS. Due to this, stand-alone ion mobility spectrometers are light enough for field applications, such as detection of chemical warfare agents [4], explosives [50], herbicides [55], pesticides [56] and organic volatile compounds [18]. IMS can also be used to detect specific compounds, such as ethanol in a fermentation process [57] or volatile compounds in food [58, 59], or identifying chemical classes of biologically relevant compounds, such as lipids, peptides and carbohydrates [60]. IMS instruments can also be used as detectors for GC [61]. The main applications of IMS-MS instruments are in metabolomics [62, 63], glycomics [63, 64] and proteomics [20, 49, 66]. Recently, TWIMS and IMS-MS instruments have been used to identify contaminants and additives in crude oil and gasoline samples, respectively [67, 68]. IMS-MS has been used to study the shape of model aromatic compounds that can be present in crude oils [69] and TWIMS has been used to produce information about sizes and shapes of compounds in the asphaltene fraction of crude oil [70].

In Table 1 are examples of situations where IMS is capable of separating isomers, e.g. hydrocarbons [71, 72], dihalogenated benzenes [73], terpenes [74] and anilines [75]. Isomers can be separated in IMS because they usually have different shapes and therefore different collision cross-sections. IMS separation before MS detection has been used to distinguish isomeric hydrocarbons [76] and polycyclic aromatic hydrocarbons [43], and to separate stereoisomers, such as *cis*- and *trans*-conformations of singly and doubly charged tryptic peptides [77]. However, it has been reported that singly protonated $[M+H]^+$ ions of two peptide isomers do not necessarily have large enough differences in their shapes, and therefore they cannot be separated by IMS, but the doubly charged $[M+2H]^{2+}$ ions of the same peptides can be [78]. Ionization of isomeric analytes can sometimes be enhanced by forming adducts (e.g. sodium, potassium or metal ions), which can be separated by IMS. For example, this has been done with sodium adducts of disaccharide-aldodols and trisaccharides [79], with

sodium, potassium and silver adducts of flavonoid diglycosides [80] and with sodium, silver, cobolt, copper, mercury and lead metal cation adducts of stereoisomers of methyl galactoside [76]. Separation of enantiomeric model compounds can be done by adding chiral modifiers (e.g. (S)-(+)-2-butanol) in the drift gas stream [81, 82]. The modifier reduces the drift time of both enantiomers, but for one enantiomer it is reduced more than for the other, which is assumed to be due to stronger interaction between the chiral centre of the enantiomer and the modifier. The TWIMS instrument has been used, e.g., to separate $[M+H]^+$ ions of the isomeric 4-butylaniline and *N*-butylaniline [83], and in protein analysis [84]. In another study, it was observed that model isomeric steroid pairs of estradiols, androsterones and testosterones showed hardly any separation with TWIMS, but their *p*-toluenesulfonyl isocyanate derivatives resulted in better separation of α- and β-estradiols, 3α- and β-androsterones and 17β- and 17α-testosterones [85].

Table 1. Examples of isomeric compounds separated with IMS, FAIMS and TWIMS.

Compound	Drift gas and separation conditions	Ionization	IMS instrumentation	Ref
Hydrocarbons	air	Radioactive, APCI and APPI	IMS-FP[a]	[71,72]
Dihalogenated benzenes	air	Radioactive, APCI and APPI	IMS-FP[a]	[73]
Terpenes	air	Radioactive, APCI and APPI	IMS-FP[a]	[74]
Anilines	air	Radioactive, APCI and APPI	IMS-FP[a]	[75]
Hydrocarbons	[b]	ESI	IMS-MS	[76]
PAH	N_2	APPI	Trapped IMS-MS	[43]
Tryptic peptides	He	ESI	IMS-MS	[77]
Peptides	N_2[c]	ESI	IMS-MS	[78]
Saccharides	N_2; Sodium adducts	ESI	IMS-MS	[79]
Flavonoid diglycosides	N_2; Cation adducts	ESI	IMS-MS	[80]
Model compounds	N_2; Chiral modifier	ESI	IMS-MS	[81, 82]
Hydrocarbons	N_2	APPI	DMS-MS	[86]
Disaccharide	N_2; Cation adducts[d]	ESI	FAIMS-MS	[87]
Phthalic acids	N_2 or CO_2	ESI	FAIMS-MS	[88]
Model aniline compounds	Ar or CO_2	ESI	TWIMS	[83, 89]
Protein	N_2	nano-ESI	TWIMS	[84]
Steroids	N_2 or CO_2[e]	ESI	TWIMS	[85]

APCI, Atmospheric pressure chemical ionization; APPI, Atmospheric pressure photoionization; ESI, Electrospray ionization; IMS-MS, Ion mobility spectrometer – mass spectrometer; DMS-MS, Differential mobility spectrometry (= also FAIMS); TWIMS, Traveling wave ion mobility spectrometry; PAH, Polycyclic aromatic hydrocarbons; N_2, nitrogen; He, Helium; CO_2, carbon dioxide; Ar, Argon; [a] IMS-MS is used to confirm ion structures; [b] Metal cations Na^+, Ag^+, Co^{+2}, Cu^{+2}, Ca^{+2}, Hg^{+2} and Pb^{+2}; drift gases He, N_2, Ar and CO_2; [c] Doubly charged ions are separated; [d] Cations studied were H^+, NH_4^+, Li^+, Na^+, K^+, Rb^+, and Cs^+; [e] *p*-toluenesulfonyl isocyanate derivatives of steroids

1.2 Basic operation principles and applications of two-dimensional gas chromatography – time-of-flight mass spectrometry

Two-dimensional gas chromatography (GC×GC) is similar to the conventional one-dimensional gas chromatography (GC) in the sense that the analyte compounds are separated in the gas phase by their interactions with a stationary phase on the column surface. The GC and GC×GC have three main components: (i) injector, (ii) column (inside the oven) and (iii) detector. The main additional parts in GC×GC are a modulator and a second column, which are located between the first column and the detector (Figure 4).

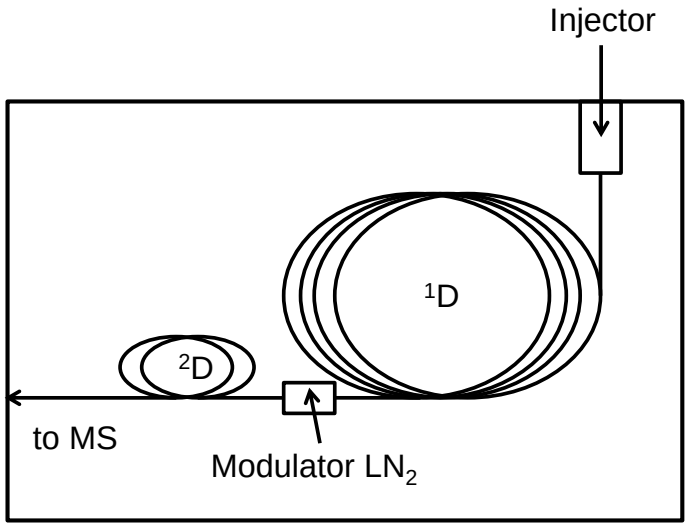

Figure 4. Schematic diagram of a two-dimensional GC×GC instrument. Modulator LN_2 = cryogenic modulator which uses liquid nitrogen as a cold jet.

There are various GC injectors for different kinds of samples. The split-splitless injector type is the most common due to the possibility to switch between two modes allowing for a wide concentration working range: split mode for highly concentrated or dirty samples and splitless mode for trace level analysis.

GC columns for GC×GC have many options with different length, diameter and film material (stationary phase). A large amount of different materials and their combinations are available for stationary phases, but generally non-polar columns are suitable for separation of non-polar compounds and polar columns for separation of polar compounds. The separation in non-polar ^{1}D column may be explained by the boiling point of the analyte. For example, 2,2-dimethylpropane with a more spherical shape has a lower boiling point (282.6±0.5 K) than pentane with a linear shape

(309.2±0.2 K), and therefore they are separated in ^{1}D. In a semi-polar ^{2}D column the separation is driven by interactions between analytes and the stationary phase of the column, where the polarity of the molecule has commonly a key role. A common combination of columns is a non-polar in the first dimension (^{1}D) column and a semi-polar in the second dimension (^{2}D) column [90]. After the separation in the ^{1}D column the sample compounds are continuously introduced by the modulator during the chromatographic run into the ^{2}D column for further separation. Different kinds of modulators are available, and they are described elsewhere [90]. In a cryogenic modulator the sample compounds are held and then released, with a cold and a hot jet, resulting in a two-dimensional separation field (Figure 4) [91].

Typical carrier gases are nitrogen, argon, helium, hydrogen and air. Linear velocity of the carrier gas has an important role in the efficiency of the chromatographic separation. Golay plots and van Deemter curves for each carrier gas are used to demonstrate the optimal linear velocities against the number of theoretical plates (resolution). For instance, hydrogen has the longest linear velocity range, but it is an expensive and flammable gas. Helium has the second longest linear velocity range after hydrogen, and therefore it is selected for applications, where a wide variety of compounds are to be analyzed with the same GC setup.

For GC×GC, MS is a common detector, especially time-of-flight mass spectrometry (TOF-MS), which has the advantage of producing full mass spectral data with high frequency to ensure a sufficient number of data points for a good peak shape.

Different detectors can be attached to GC×GC, for example a flame ionization detector (FID). It is cheap, easy to maintain, and good for quantitative analysis with a large linear response range for organic compounds.

In most GC×GC-MS instruments the analytes are ionized after the ^{2}D separation by electron ionization (EI, 70 eV). The electrons collide with analyte molecules by knocking out an electron, and typically molecular ions $M^{+\cdot}$ and their fragments are observed. EI is a stable and repeatable ionization technique with already existing large mass spectral libraries; the most important is the one by the National Institute of Standards and Technology (NIST) [92].

GC×GC instruments have a high peak capacity [8], and therefore they are good for many kinds of applications in different fields of chemistry, such as environmental [93], food [94], metabolomics [95, 96], biological [97] and geological [98]. GC×GC is an

attractive tool for difficult analytical applications, and it is a good tool for screening complex samples in order to find compounds such as illegal drugs [99] and anabolic agents in doping control [100] and crude oil samples [101].

GC×GC-TOF-MS has been used in petroleum research to analyze different kinds of samples, the examples of which are presented in Table 2.

Table 2. Examples of petroleum studies with GC×GC-TOF-MS.

Research topic	Reference
Fischer-Tropsch reaction	[102]
Extra heavy gas oil	[103, 104]
Heavy petroleum fraction	[105, 106]
Crude oils from Ceará Basin	[107]
Biodegradation of oils	[108-110]
Depositional paleoenvironmental conditions	[111-113]
Maturation of oils	[114]
Trace analysis	[115]
Modified white gasoline	[116]
Higher plant biomarkers in oils and rock extracts	[101]
Marine diesel fuel	[117]
Petroleum contaminated sediment	[98]
Sulfur compounds in diesel oils	[118]

In oil research, Fourier transform ion cyclotron resonance mass spectrometry (FT-ICR-MS) is also an important instrument, which has been commonly used to analyze polar crude oil fraction or whole oil [119, 120]. In FT-ICR, without chromatographic separation, the geochemical evaluation is conducted based on accurate mass data, which can be used to determine the chemical compositions of each mass peak observed [121, 122]. However, the isomers with the same chemical composition are not distinguished.

An interesting compound group present in all crude oils are biomarkers that originate from living organisms which populated the earth a long time ago. They reflect different kinds of initial organic input material, environmental and diagenesis conditions, maturation and biodegradation during the crude oil formation process [123, 124].

Crude oil contains many isomeric hydrocarbons and the examples of important studies where isomers have been separated by GC×GC are illustrated in Table 3. Many of these isomers share the same retention time in ^{1}D, and also share the same exact mass. These co-eluting isomers can be separated sometimes in ^{2}D, for example C_{24} tricyclic terpane and C_{24} demethylated tricyclic terpane, and C_{30}R 25-norhomohopane

and C_{30} hopane are separated [108]. In some cases isomeric compounds have an increase in retention time in both ^{1}D and ^{2}D, for example the isomers of alkyl tetramantane [114]. The most important factors for isomer separation in GC×GC are the different properties of the stationary phase of the columns used.

Table 3 Examples of studies where isomers have been separated in petrochemical samples with GC×GC.

Isomers	**GC×GC column**	**Ref**
C_{19}–C_{24} tricyclic terpanes	*HP-5 and BPX-50	[112]
C_{27}-C_{29} steranes	*HP-5 and BPX-50	[112]
C_{31}-C_{35} hopane	*HP-5 and *BPX-50	[108, 112]
Oleanane	*HP-5 and *BPX-50	[124]
Alkyl tetramantanes	*HP-5 and *BPX-50	[114]
Branched alkanes	*HP-1 and BPX-1701	[98, 117]
Alkylcycloalkanes	*HP-5 and BPX-50	[125]
Dibenzothiophenes	*HP-5 and BPX-50	[113]
Triaromatic streroids	*HP-5 and BPX-50	[113]
Alkylpyrenes	*HP-5 and BPX-50	[104]

* The column where separation of isomers occurred.

1.2 Aims of the study

The first part of the thesis discusses a negative mobility standard for IMS (Paper I), the separation of different ion structures with IMS (Paper II) and the factors affecting the separation of isomers in linear drift tube IMS (Papers I-III). The second part of the thesis discusses the geochemical assessment of Recôncavo Basin, Brazil (Paper IV) and new biomarkers detected with GC×GC-TOF-MS in Brazilian crude oils (Paper V).

The specific aims of the thesis were the following:

- Search for new negative IMS mobility standard by analysing sterically hindered phenols with negative APCI-IMS (Paper I)
- Separate different ion structures of pyridine and naphthol compounds with positive APPI-IMS (Paper II)
- The capability of IMS to separate isomers was studied with two phenolic (Paper I), two naphthol (Paper II) and eight amine (Paper III) isomers.
- During the analysis, new peaks were observed in the IMS spectra. MS was applied to the study of the identity of these peaks (Papers I-III)
- Distinguishing minor geological differences in the Recôncavo Basin (oil field), Brazil, with GC×GC-TOF-MS using β-carotane and other biomarkers (Paper IV)
- Geochemical evaluation of selected Brazilian crude oils with GC×GC-TOF-MS. Novel biomarkers were detected during the analysis and their tentative identification and geochemical significance were studied (Paper V).

2. EXPERIMENTAL

2.1 Chemicals

The solvents and gases used in the thesis are presented in Table 4, the analytes in Table 5 and analyte structures in Figures 5 and 6. All the analytes in the IMS experiments (Papers I-III) were first dissolved in solvents, according to Table 4, to achieve 5 mM stock solutions, which were further diluted to give 50 µM, 100µM and 500 µM working concentrations. The isomeric amines studied in Paper III (Figure 6) were diluted further with methanol:toluene (95:5%) to give 50 and 100 µM solutions and following mixtures were prepared: Mix A (2,4,6-Col, *N*,*N*-DMA, *n*-M-*o*-T and 2-MBA), Mix B (PEA, 4-EA and 2,6-D*t*BPyr) and Mix C (2-, 3-, 4-MBA, and 2,6-D*t*BPyr).

Table 4. The solvents and gases used in this thesis.

Solvent / gas	**Purity**	**Manufacturer**	**Paper**
Acetonitrile		Lab-Scan, Dublin, Ireland	I
n-Hexane	>95%	Poch SA, Gliwice, Poland	I & II
n-Pentane	>99%	Fluka, Steinheim, Germany	II
Methanol	HPLC grade	Baker, Deventer, Holland	II
Toluene	HPLC grade	Lab-Scan, Dublin, Ireland	II
Toluene	HPLC grade	Baker, Deventer, Holland	III
Methanol	HPLC grade	Lab-scan, Dublin, Ireland	III
Dichloromethane, *n*-hexane and methanol	Chromatographic grade	Tedia, Rio de Janeiro, Brazil	IV & V
Nitrogen	NGLCMS20 nitrogen generator 99.5%	Labgas Instrument Co., Espoo, Finland	I-III
Bottled air (80% N_2, 20% O_2)	4.0	AGA Ltd., Espoo, Finland	I

Table 5. The standards used in this thesis. All the standards were purchased from Sigma-Aldrich (Steinheim, Germany) unless otherwise stated.

Paper I	**Abbreviation**	**Solvent / dopant**	**Purity (%)**
2-*tert*-Butylphenol	2-*t*BPh	Hexane	>99
2,4-Di-*tert*-butylphenol	2,4-D*t*BPh	Hexane	>99
2,6-Di-*tert*-butyl-4-methylphenol	2,6-D*t*B-4-MPh	Hexane	>99
2,4,6-Tri-*tert*-butylphenol	2,4,6-T*t*BPh	Hexane	>98
2,4,6-Trinitrotoluene[a]	2,4,6-TNT	Acetonitrile	99
2,6-Di-*tert*-butylpyridine	2,6-D*t*BPyr	Hexane	>97
Paper II			
Pyridine[b]		Hexane and hexane:toluene (90:10%)	>99.5
1-Naphthol		Hexane and hexane:toluene (90:10%)	>97
2-Naphthol		Hexane and hexane:toluene (90:10%)	>97
2-*tert*-Butylpyridine	2-*t*BPyr	Hexane and hexane:toluene (90:10%)	>97
2,6-Di-*tert*-butylpyridine	2,6-D*t*BPyr	Hexane and hexane:toluene (90:10%)	>97
2,6-Di-*tert*-butyl-4-methylpyridine	2,6-D*t*B-4-MPyr	Hexane and hexane:toluene (90:10%)	>98
Paper III			
2,4,6-Collidine[b]	2,4,6-Col	Methanol:toluene (95:5%)	>99
N,N-Dimethylaniline	*N,N*-DMA	Methanol:toluene (95:5%)	>99.5
N-methyl-*o*-Toluidine	*n*-M-*o*-T	Methanol:toluene (95:5%)	>95
2-Phenethylamine	PEA	Methanol:toluene (95:5%)	>99
4-Ethylaniline	4-EA	Methanol:toluene (95:5%)	>98
2-Methylbenzylamine	2-MBA	Methanol:toluene (95:5%)	>96
4-Methylbenzylamine	4-MBA	Methanol:toluene (95:5%)	>97
3-Methylbenzylamine	3-MBA	Methanol:toluene (95:5%)	>98
2,6-Di-*tert*-butylpyridine	2,6-D*t*BPyr	Methanol:toluene (95:5%)	>97
Papers IV-V			
n-tetracosane-D_{50}[c]		Dichloromethane	>98%
pyrene-D_{10}[c]		Dichloromethane	

[a] *Supelco* (Bellefonte, PA, USA), [b] Merck (Darmstadt, Germany) and [c] Cambridge Isotope Laboratories, Andover, MA, USA.

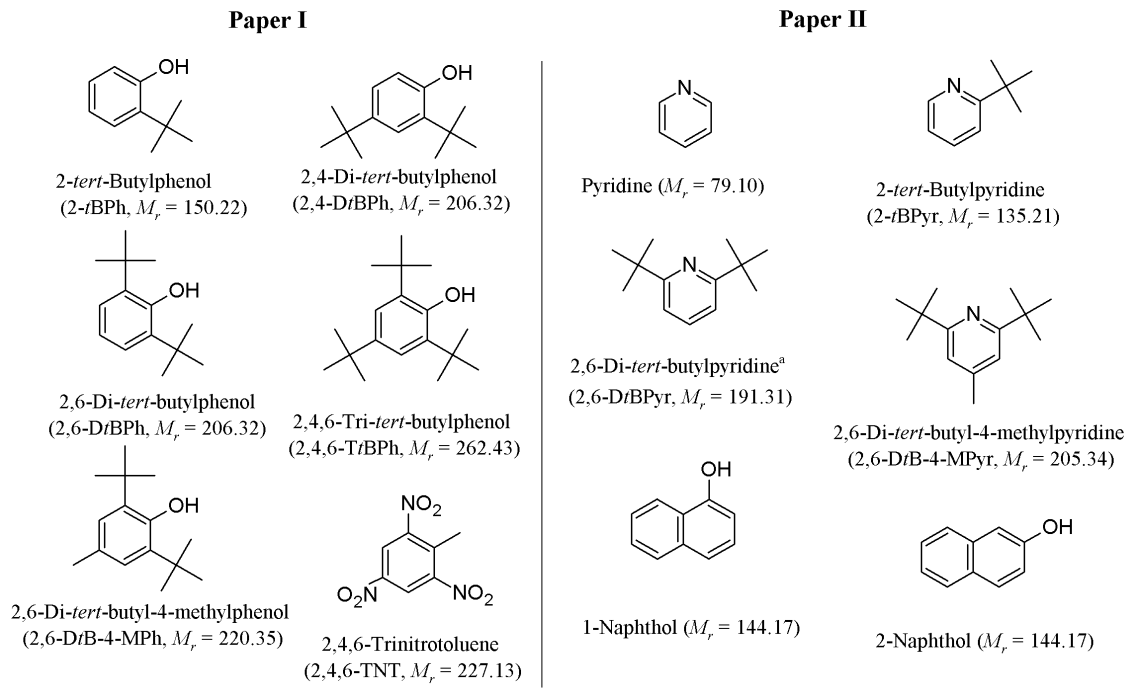

Figure 5. Compounds studied with IMS in Papers I and II. [a] = also studied in Papers I and III (modified from ref. [127]).

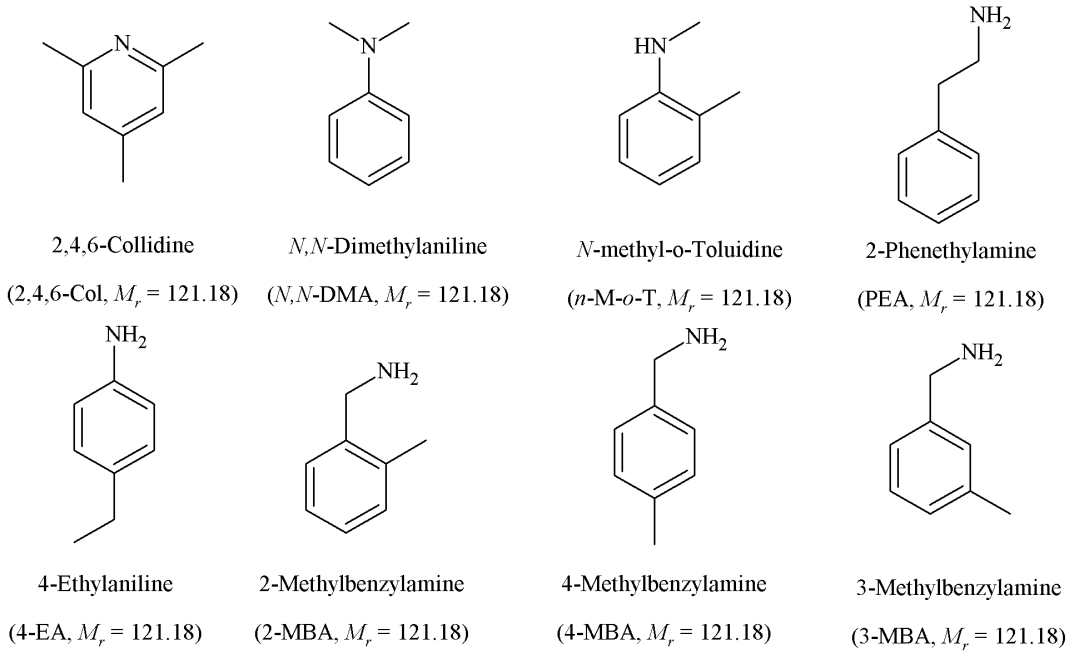

Figure 6. Isomeric amines studied with IMS in Paper III.

2.2 Oil fractioning (Papers IV-V)

The procedure for fractioning 20 crude oil samples in Paper IV was adopted from ref. [128]. Briefly, the LC fractionation was conducted by using a vertical glass column in atmospheric pressure to separate saturated, aromatic and polar fractions from crude oil. Approximately 100 mg of each oil sample was weighed with a calibrated analytical balance (± 0.1 mg) and dissolved in 500 µL of a dichloromethane solution with internal standard *n*-tetracosane-d_{50} at a concentration of 100 µg L^{-1}. This sample solution was placed on the top of a glass column (dimensions 13 × 1 cm) packed with 3 g of Silica Gel 60 (particle size from 0.063 to 0.200 nm, Merck, Darmstadt, Germany), which was previously purified with hexane and activated in an oven at 120 °C for 12 hours. The samples were eluted into different fractions in the following order; saturated hydrocarbons with *n*-hexane (10 mL), aromatic hydrocarbons with *n*-hexane:dichloromethane (80:20%, 10 mL) and polar compounds with 10 mL of dichloromethane:methanol (90:10%, 10 mL). The fractions were collected in 50 mL flasks, and the solvent was evaporated by a rotary evaporator under reduced pressure. Each fraction was then transferred to a 2 mL vial (pre-weighed) using dichloromethane, which was subsequently evaporated under a nitrogen gas flow (from bottle), after which the vial was weighed again. In the Paper V the 11 crude oil samples crude oils, from the north to the south regions of Brazil, were pre-fractionated to saturated hydrocarbon and aromatic fractions by CENPES (Centro de Pesquisas e Desenvolvimento Leopoldo Américo Miguez de Mello, Rio de Janeiro, Brazil). They were also classified by CENPES using proprietary classifying methods (Table 1).

2.3 Separation of n-alkanes from branched and cyclic saturated hydrocarbons by urea adduct formation (Papers IV-V)

In order to separate *n*-alkanes from branched (B) and cyclic (C) saturated hydrocarbon in the saturated hydrocarbon fraction, urea adducts of *n*-alkanes were formed, as has previously been presented in references [128, 129]. The saturated hydrocarbon fraction was dissolved in 1000 µL of *n*-hexane and a 500 µL aliquot was transferred to a test tube of 18×180 mm. 1 mL of acetone and 1 mL of *n*-hexane were added to the test tube, and the mixture was vortexed. To prepare a saturated solution of

urea, 30 g of urea was dissolved in 100 mL of methanol. The solution was stored in a refrigerator at 8 ° C. 1 mL of the saturated urea solution was added slowly to the test tube containing the saturated hydrocarbon fraction, and the immediate precipitation of urea crystals was observed. The test tube was heated in a water bath at 50 ° C to dissolve all the crystals and then cooled to room temperature for recrystallization of the urea. The crystallization was terminated in a freezer at -20 °C for 12 hours. After this, the solvent was evaporated under a nitrogen flow to obtain dried crystals, which were rinsed five times with 2 mL of *n*-hexane. The supernatant containing the B/C fraction, was transferred into a 30 mL balloon. The solvent was evaporated under reduced pressure and the urea crystals were dissolved in distilled water. To obtain the branched and cyclic hydrocarbon (B/C) fractions, liquid-liquid extraction of urea crystals was carried out with 2 mL of *n*-hexane. The organic layer was transferred to a 30 mL flask with a Pasteur pipette. This extraction step was repeated five times. The solvent was evaporated under reduced pressure and the B/C fraction was transferred to a previously weighed 2 mL vial and weighed again. The residue was dissolved in 500 µL of dichloromethane.

2.4 Ion mobility spectrometry instrumentation (Papers I-III)

Measurements with IMS were conducted with a custom-made cylinder drift tube ion mobility spectrometry attached to a Sciex API300 triple quadrupole MS (Applied Biosystems-SCIEX, Concord, Ontario, Canada), which is referred to as IMS-MS (Figure 8), and with a similar drift tube attached to a faraday plate detector, which is referred to as IMS-FP. A more detailed description of these instruments can be found elsewhere; IMS-MS [44] and IMS-FP [29]. Briefly, both drift tubes have a similar design and the ion sources used in this study could be applied in both of the IMS instruments. The measurement parameters are summarized in Table 6.

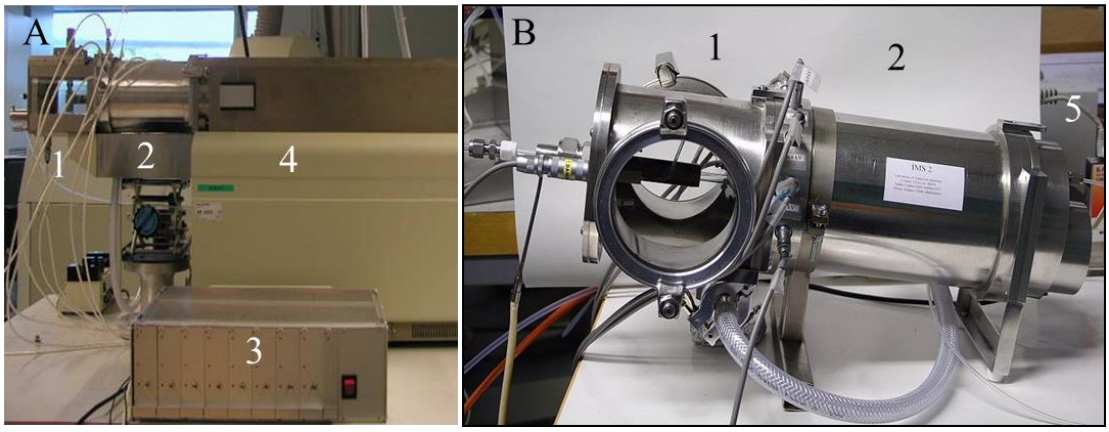

Figure 8. IMS connected to API300 MS (A) and to faraday plate detector (B): (1) ion source, (2) IMS drift tube, (3) control unit for IMS, (4) Sciex API300 triple quadrupole MS and (5) faraday plate (modified from ref [127]).

Table 6. Summary of IMS and MS parameters used in the study. The drift gas was nitrogen in all experiments, except in Paper III some of the experiments were carried out by using gas mixtures with varying proportions of nitrogen:argon and nitrogen:helium.

Parameter	(Paper I)	(Paper II)	(Paper III)
MS			
Declustering potential (V)	15-25	20-30	5
Focusing potential (V)	180-200	130-220	130
Entrance potential (V)	5		
IMS-MS			
Drift length (cm)	13.3		
Desolvation length (cm)	7.65		
Drift flow (L/min)	~2.4		
Gate opening time (µs)	300		
Drift field (V/cm)	270-378	316-363	316
Desolvation field (V/cm)	230-260	272-303	304
Reflector plate in APPI experiments (kV)		0.8-1.6	1
Needle voltage[1] (V)	1.3-1.5		
Needle voltage[2] (V)	1.7-2.2		
IMS-FP			
Drift length (cm)	-	13.85	
Desolvation length (cm)	-	7.65	
Dirft flow (L/min)	-	2.1	1.9-2.5
Gate opening time (µs)	-	100	200
Drift field (V/cm)	-	378	316
Desolvation field (V/cm)	-	378	316
Reflector plate in APPI experiments (kV)	-	2	
Needle volt. APCI (V)	-		2.0-2.2

[1] nebulizer gas was nitrogen, [2] nebulizer gas was air (80:20 nitrogen:oxygen).

The IMS-MS instrument was operated either at full scan mode, typically a mass range of *m/z* 30-300 or 50-500, or with selected ion monitoring (SIM) mode. In the MS full scan mode, both B-N gates in the IMS were open, and in SIM mode the gates were pulsed to obtain a mobility window, which is described in more details [44]. The drift times of two ions were typically monitored simultaneously. The gates and voltage of IMS were controlled by a LabVIEW (National Instruments, Austin, US) based on a custom-made program, and the data was collected with Analyst 1.4.1 (Applied Biosystems/MDS SCIEX, Concord, ON, Canada). The data was further processed with Microsoft Excel 2002 (Microsoft Corporation, Redmond, WA, USA) applying Equation

(4) to calculate reduced mobilities. The IMS-FP instrument was operated with one B-N gate. A similar custom-made program as used in IMS-MS was also used to control the IMS-FP instrument and data processing to combine 2000 mobility spectra together. The data was further processed in ChemStation rev. 10.02 (Agilent Technologies, Inc., Palo Alto, CA, USA) with custom-written macros to calculate reduced mobility values.

A custom-made heated nebulizer was used to transfer the liquid sample to gas phase [29, 43, 130]. A syringe pump was used to deliver the liquid sample flow at a steady speed of typically 120-180 µL/h to the nebulizer (nitrogen or air) gas flow.

The nitrogen gas for the nebulizer and drift gas was produced from compressed air and is described in Papers I and II. Additional measurements in Paper I were conducted using bottled air (80:20 % nitrogen:oxygen) as the nebulizer gas. Mainly, all the experiments were carried out nitrogen being the drift gas. Only some of the experiments in Paper III were carried out by using gas mixtures of nitrogen:argon and nitrogen:helium. All the measurements were conducted at ambient pressure, which was monitored with a pressure meter (Series 902; MKS Instrument, Andover, MA, USA).

2.5 Temperature of ion mobility drift tube (Paper I)

Most of the experiments were performed at room temperature, and when the drift tube was heated the temperature was calculated using 2,6-di-*tert*-butylpyridine as a thermometer compound. Briefly, since 2,6-DtBPyr is a sterically hindered and inert molecule, it has linear temperature dependence [12]. Taking into account that the mobility of a compound is proportional to temperature (Equation 4) when other parameters except T and t_d are constant, the Equation 4 can be reduced to Equation 5:

$$K \propto \left(\frac{273}{T} \right) \tag{5}$$

Where K is the mobility of 2,6-DtBPyr.

The mobility value of 2,6-di-*tert*-butylpyridine without temperature and pressure correction measured in our laboratory, $K_{2,6\text{-DtBPyr}} = 1.63$ cm^2/Vs, at the room temperature (296 K). This was used as the calibration point for the calculations for the temperature range (296-335K) of the IMS drift tube.

2.6 Two-dimensional gas chromatography – time-of-flight mass spectrometry instrumentation (Papers IV-V)

The GC×GC-TOF-MS analyses were performed using the same instrumental setup as in the references [112, 131] using a Pegasus 4D (Leco, St. Joseph, MI, USA) GC×GC-TOF-MS, composed of an Agilent 6890 GC (Palo Alto, CA, USA) equipped with a secondary oven, a cryogenic modulator which uses liquid nitrogen for the cold jet and a Pegasus III (Leco, St. Joseph, MI, USA) TOF-MS (Figure 7). A DB-5 column (Agilent Technologies, Palo Alto, CA, USA), containing 5% phenyl–95% methylsiloxane (30 m, 0.25 mm i.d., 0.25 µm d_f) was used as the first dimension column (^{1}D). A BPX-50 column (SGE, Ringwood, VIC, Australia), containing 50% phenyl–50% methylsiloxane (1.5 m, 0.1 mm i.d., 0.1 µm d_f) was used as the second dimension column (^{2}D). The ^{2}D column was connected to the TOF-MS inlet by a 0.5 m x 0.25 mm i.d. uncoated deactivated fused silica capillary, SGE mini-unions and Siltite™ metal ferrules of 0.1–0.25 mm i.d. (Ringwood, VIC, Australia).

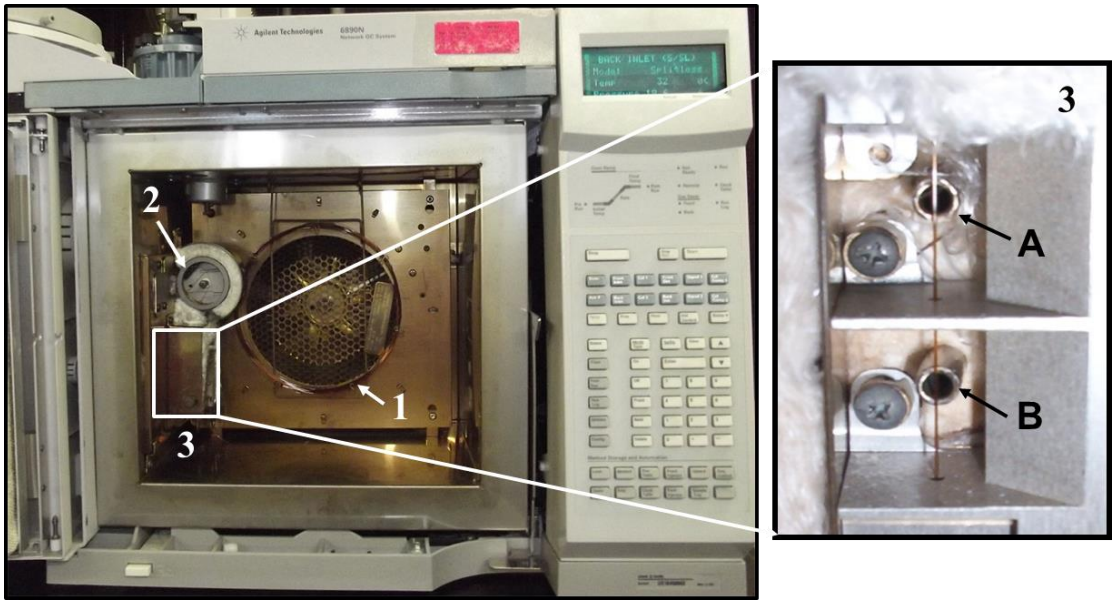

Figure 7. Modified GC oven: (1) ^{1}D GC column, (2) added ^{2}D oven and the ^{2}D GC column and (3) cryogenic modulator between the two columns (A and B are tubes for cold and hot jets); in the small figure (3) the cryogenic modulator is rotated 90° towards the door of the GC oven.

The GC conditions for the ^{1}D include: splitless injection of 1 µL at 290 ºC, purge time of 60 s, and purge flow of 5 mL/min. Helium was used as the carrier gas at a constant flow rate of 1.5 mL/min. The primary oven temperature program began at 70 ºC for 1 min, and was then increased to 170 ºC at 20 ºC/min, and further to 325 ºC at 2 ºC/min. The secondary oven temperature program was 10 ºC higher than the primary one. The modulation period was 8 s with a 2 s cold and hot pulses, and the cryogenic modulator temperature was set 30 ºC higher than the primary GC oven temperature program. The transfer line to the MS was set at 280 ºC, the electron energy in electron ionization (EI) was 70 eV, the mass range was *m/z* 50–600 and the ion source temperature 230 ºC. The detector was always set +50 V above the daily measured auto-tune value, and the acquisition rate was 100 spectra/s. Compound identification was performed by a comparison of mass spectra, retention time and elution order with data published in the literature.

2.8 Principle component analysis (Papers IV-V)

The software package Statistica 8 (Statsoft Inc.) was used in all statistical calculations in this work. Principal Component Analysis (PCA) was based on the covariance matrix. All variables were mean centered and scaled by the sample standard deviation. 42 geochemical parameters from 20 samples reported in Tables 10 and 11 (Paper IV) were used to create a matrix of the petroleum system in Recôncavo Basin. 42 parameters of maturity and source from 11 samples reported in Tables 12 and 13 (Paper V) were used to study correlations. Also these same 11 samples were evaluated by analysis of 101 normalized peak areas: area of compounds / area of internal standard (A_c/A_{is}).

3. RESULTS AND DISCUSSION

3.1 Behavior of sterically hindered phenols in IMS-MS (Paper I)

In Paper I, gas phase mobility properties of phenolic compounds with varying numbers of *tert*-butyl groups were studied with negative APCI-IMS-MS to determine their suitabilities as mobility standards (Figure 5). 2,4,6-trinitrotoluene was also included in this study as it has been used previously as a reference compound [18], and its behavior has been studied in more detail after our study [31]. The same set of phenolic compounds as used in this study has not been reported earlier in IMS literature.

The measured mass spectrometric data show that all the compounds produced deprotonated $[M-H]^-$ molecules. In the negative ion APCI mass spectra measured for 2-*t*BPh an oxygen insertion ion $[M-H+O]^-$ at *m/z* 165 was observed, in addition to the $[M-H]^-$ ion at *m/z* 149. When air was used as the nebulizer gas, instead of nitrogen, this oxygen insertion ion was observed more clearly. A similar observation was made for 2,4,6-TNT, since the oxygen adduct $[M+O]^-$ ion at *m/z* 243 was seen more clearly when the nebulizer gas was air. Table 7 illustrates other typical ions produced by 2,4,6-TNT: $[M-NO]^-$ at *m/z* 197, $[M-H]^-$ at *m/z* 226, M^- at *m/z* 227, and with a lower intensity $[M-OH]^-$ at *m/z* 210. All these 2,4,6-TNT ions observed are in line with ions reported in the literature [17, 31, 132]. In addition, ions at *m/z* 183 and 213 were observed sometimes in full scan MS spectra in the presence of the oxygen adduct ion. The formation of these ions could therefore be due to loss of one or two NO groups from the oxygen adduct

ion. However, in a recent article it was reported that the ion at *m/z* 213 is 1,3,5-trinitrobenzenanion, which is produced in the degradation of 2,4,6-TNT by ozone in an APCI ion source [133]. With the current data, it is not possible to conclude which explanation is correct.

The absolute reduced mobilities of selected identified analyte ions, at room temperature, are summarized in Table 7. Analytes produced more than one mobility peak due to dimerization or adduct formation. The variations in mobility values were typically <2%. The reduced mobility value of 2,4,6-TNT ion $[M-H]^-$ is within 2% agreement with values presented at the literature [31].

Table 7. Summary of reduced mobilities K_0 (cm^2/Vs) measured with negative APCI-IMS-MS with nitrogen as the nebulizer gas. The standard compounds were dissolved in hexane, unless otherwise stated. The numbers represent the peak numbers in the order they appear in the mass-selected mobility spectra. The structures of the standard compounds are presented in Figure 5 (adapted from Paper I).

Compound	Mass (u)	Ion formula	Measured ion, *m/z*	1st (K_0)	2nd (K_0)	3rd (K_0)	4th (K_0)
2-*t*BPh	150	$[M-H+O]^-$	165[a]	1.63	1.13[b]		
		$[M-H]^-$	149	1.63	1.53	1.14[b]	
2,4-D*t*BPh	206	$[M-H]^-$	205	1.34	1.29		
2,6-D*t*BPh	206	$[M-H]^-$	205	1.43	1.37		
2,6-D*t*B-4-MPh	220	$[M-H]^-$	219	1.36	1.29		
2,4,6-T*t*BPh	262	$[M-H]^-$	261	1.23	1.18		
2,4,6-TNT	227	$[M+O]^-$	243[a,c]	1.53			
		M^-	227[c]	1.58[d]	1.53	1.35	
		$[M-H]^-$	226[c]	1.58	1.48	1.36	
		$[M-OH]^-$	210[c]	1.53			
		$[M-NO]^-$	197[c]	1.64	1.53	1.42	1.36

[a] nebulizer gas was air; [b] dimer; [c] solvent ACN; [d] most likely the ^{13}C isotope peak of the ion at *m/z* 226

The compounds 2,6-D*t*BPh (Figure 9A), 2,6-D*t*BP-4-MPh and 2,4,6-T*t*BPh showed similar mobility peak patterns with two relatively large mobility peaks (Table 7). One requirement for the IMS instrumental standard is that the mobility value is independent of the IMS drift field. Therefore in our study, the variation in drift field (270-344 V/cm) was also tested for these three phenolic compounds. It was observed that all the reduced mobility values remained the same within the experimental error. However, the temperature variation (296-335 K) study done for 2,6-D*t*BP-4-MPh and 2,4,6-T*t*BPh showed that the intensity of the peak with a higher mobility value (1st peak in Table 7)

increased when the temperature increased. This is an indication that at least the lower mobility peak (2nd peak in Table 7) is an adduct ion, for example an adduct with O_2 or NO_x. However, no adducts were observed in the measured mass spectra. This is likely as they dissociate in the MS interface.

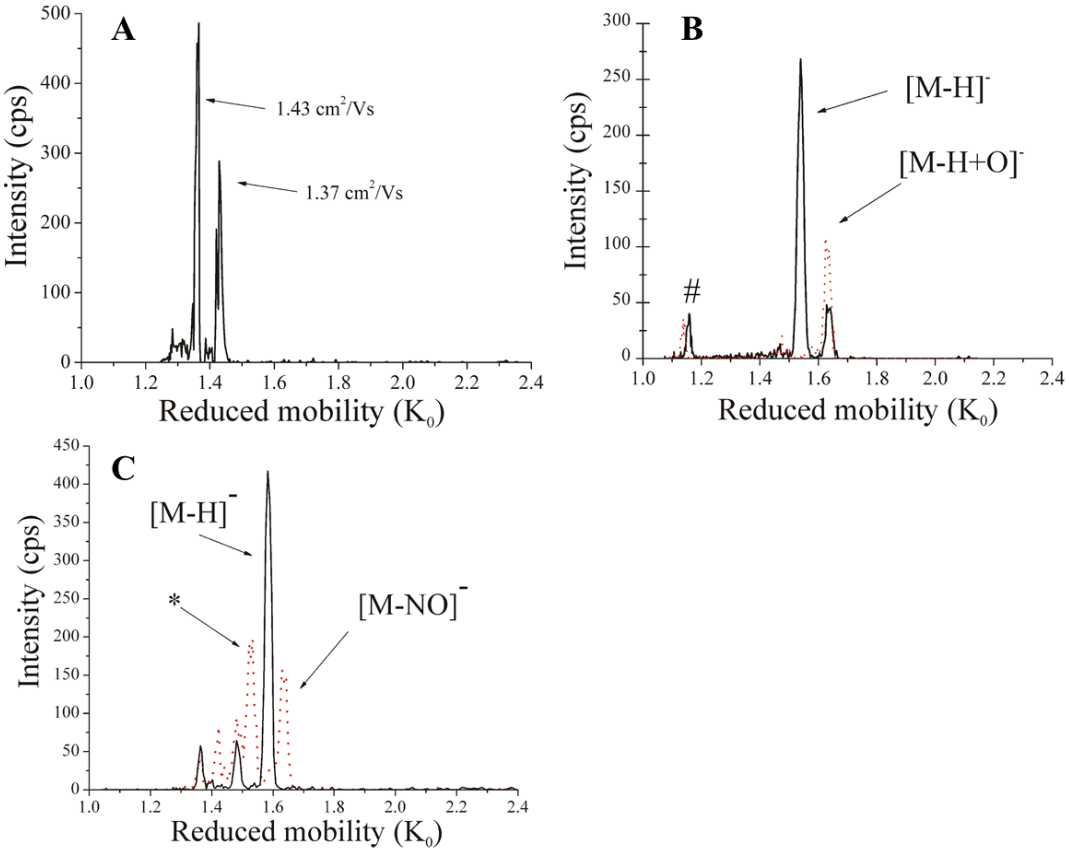

Figure 9. Negative APCI-IMS-MS mass-selected ion mobility spectrum of (A) $[M-H]^-$ ion of 2,6-D*t*BPh at *m/z* 205, (B) $[M-H]^-$ and $[M-H+O]^-$ ions of 2-*t*BPh at *m/z* 149 (solid line) and *m/z* 165 (dotted line), respectively, (C) $[M-NO]^-$ and $[M-H]^-$ ions of 2,4,6-TNT at *m/z* 197 (2nd peak is marked with asterisk, dotted line) and *m/z* 226 (solid line), respectively. The measurements were carried out in room temperature (296 K) using nitrogen as the drift and nebulizer gases (A, C) and using nitrogen as the drift gas and air as the nebulizer gas (B). # most likely the analyte dimer.

The mass selected mobility spectra of the $[M-H]^-$ ion of 2-*t*BPh typically showed three peaks; one (2nd, Table 7, Figure 9B) peak due to the deprotonated molecule at *m/z* 149, another peak (1st, Table 7, Figure 9B) due to the oxygen insertion ion $[M-H+O]^-$ at *m/z* 165 and the third one (3rd, Figure 9B, marked with #) most likely due to the analyte dimer. In tandem mass spectrometric measurements the oxygen insertion ion at *m/z* 165 produced an ion at *m/z* 149 as a product ion (results not shown). Interestingly, the

oxygen insertion ion had a higher mobility than the lighter $[M-H]^-$ ion. This could be due to the fact that the $[M-H]^-$ ion exists initially as an adduct (e.g. O_2 or NO_x), which subsequently breaks down into the $[M-H]^-$ ion in the MS interface. An alternative explanation is that by the oxygen insertion a –OH group is formed in the *ortho*-position of the oxygen atom allowing for the formation of an internal hydrogen bond. Due to this, the internal hydrogen bond is shielding the charge, resulting in a decreased interaction of the $[M-H+O]^-$ ion with the drift gas compared to the $[M-H]^-$ ion.

The two isomeric compounds, 2,4- and 2,6-D*t*BPh, both had two mobility peaks in the mass-selected ion mobility spectrum of the $[M-H]^-$ ion at *m/z* 205. As can be seen from Table 7, there is a clear difference, of about 0.1 units, in the reduced mobility values of both peaks when the mobility values of these two isomers are compared. This could be because, in the case of the ionized 2,4-D*t*BPh, the charge is exposed more to interactions with the drift gas than in the case of 2,6-D*t*BPh, which has two *tert*-butyl groups shadowing the ionization site (Figure 5). It was later observed that 2,4-D*t*BPh also formed a small quantity of dioxygen adduct $[M+O_2]^-$ ions at *m/z* 238, which had the same reduced mobility (K_0 = 1.29 cm^2/Vs) as the second mobility peak of $[M-H]^-$ ion [134]. This indicates that the dioxygen adduct $[M+O_2]^-$ is initially present in the ionization chamber and is broken down after the IMS analysis to form an $[M-H]^-$ ion.

2,4,6-TNT produced several mass-selected mobility peaks (Table 7). The $[M-H]^-$ ion at *m/z* 226 showed three mobility peaks, of which the 1st peak (K_0 = 1.58 cm^2/Vs) had the highest intensity (Figure 9C). The $[M-NO]^-$ ion at *m/z* 197 produced four mobility peaks, of which the 1st and the 2nd (K_0 = 1.64 cm^2/Vs and K_0 = 1.53 cm^2/Vs, respectively) were the most intense. Interestingly, the 2nd mobility peak of $[M-NO]^-$ ion (marked with an asterisk in Figure 9C) shared the same mobility with $[M-OH]^-$ at *m/z* 210, M^- at *m/z* 227 and $[M+O]^-$ at *m/z* 243. This could be because in the drift tube the precursor ion $[M+O]^-$ moves across the drift region, forming the rest of the ions (*m/z* 197, *m/z* 210 and *m/z* 227) at the MS interface after the IMS separation. Note, that even though the mass difference of the $[M-H]^-$ and the M^- ions at *m/z* 226 and *m/z* 227, respectively, is only one mass unit, the mobility difference (K_0 = 1.58 cm^2/Vs and K_0 = 1.53 cm^2/Vs, respectively) is relatively large. This supports the interpretation that the M^- ion originates from the oxygen adduct ion $[M+O]^-$. Also the mass difference between $[M-H]^-$ and $[M+O]^-$ ions is large enough to explain the mobility difference.

In summary, two isomeric phenols, 2,4-D*t*BPh and 2,6-D*t*BPh, could be separated with IMS-MS. Three of the phenols, namely 2,6-D*t*BPh, 2,6-D*t*B-4-MPh and 2,4,6-T*t*BPh, produced typically two mobility peaks in the mass-selected mobility spectra measured for the $[M-H]^-$ ion. These three phenolic compounds behaved similarly under different measuring conditions and they could be used as instrumental standards alongside with 2,4,6-TNT. Further characterization is still required for example at higher drift tube temperatures.

3.2 Separation of different ion structures with IMS (Paper II)

The aim of the study in Paper II was to investigate the capacity of IMS to separate different ion structures of pyridine and naphthol compounds (Figure 5) in the gas phase. The ionization conditions in APPI were selected so that different ion structures, radical cation $M^{+\cdot}$ and protonated molecule $[M+H]^+$ ions, could be created for the same molecule. The MS literature has examples of how APPI can be used to produce different ion forms by altering the solvent and / or the dopant [36, 135, 136].

When the analytes (Figure 5) were dissolved in hexane, APPI produced mainly protonated molecules $[M+H]^+$ at *m/z* 145, 145, 192 and 206 for 1- and 2-naphthol, 2,6-D*t*BPyr and 2,6-D*t*-4-BPyr, respectively. However, when the analytes were dissolved into hexane:toluene (90:10%) they also produced radical cations $M^{+\cdot}$ (*m/z* 144, 144, 191 and 205). In the case of 2,6-D*t*BPyr and 2,6-D*t*-4-BPyr, the $M^{+\cdot}$ ions were observed together with unexpected dioxygen adducts $[M+O_2]^{+\cdot}$ at *m/z* 223 and *m/z* 237, respectively. Product ion mass spectra for the $M^{+\cdot}$ and $[M+O_2]^{+\cdot}$ ions of 2,6-D*t*BPyr and 2,6-D*t*B-4-MPyr produced similar fragment ions, expect that for the $[M+O_2]^{+\cdot}$ ion the first fragmentation step was the loss of O_2. For pyridine and 2-*t*BPyr, both solvents efficiently produced only protonated molecules at *m/z* 80 and 136, respectively. In addition to the $[M+H]^+$ ion, pyridine produced also a $[M+91]^+$ ion at *m/z* 170, when hexane:toluene (90:10%) was used as the solvent. Further tandem MS inspections of the $[M+91]^+$ ions structure indicated that it could be a benzyl cation adduct of pyridine.

In the next step, the absolute reduced mobilities of most of the identified analyte ions were recorded (Table 8). The mobility values for the analyte ions, obtained with hexane and hexane:toluene (90:10%) solvents, were the same. The repeatability of the mobility measurements was evaluated by measuring the mass-selected reduced mobility values

for the $[M+H]^+$ ion of 2,6-D*t*BPyr in hexane, because it has been previously used as a mobility standard [12]. The relative standard deviation for 2,6-D*t*BPyr was 0.7% (n = 13, K_0 = 1.49 cm^2/Vs).

Pyridine produced two main (1st and 2nd, Table 8) mobility peaks for the $[M+H]^+$ ion with K_0 = 2.04 (monomer) and 1.69 cm^2/Vs (dimer), when hexane was used as the solvent. Interestingly, the use of hexane:toluene (90:10%) as the solvent produced an additional 3rd peak at K_0 = 1.63 cm^2/Vs at *m/z* 80 with nearly the same mobility (1.64 cm^2/Vs) as for the $[M+91]^+$ ion at *m/z* 170. This is in line with the earlier tandem MS findings, suggesting that the *m/z* 170 ion is a benzyl cation adduct which is formed in the desolvation or ionization region of the IMS. 2-*t*BPyr produced a single mobility peak (K_0 = 1.73 cm^2/Vs) for the $[M+H]^+$ with both hexane and hexane:toluene (90:10%) solvents.

Table 8. Summary of the reduced mobilities K_0 (cm^2/Vs) measured with positive APPI-IMS-MS. The standard compounds were dissolved in hexane or hexane:toluene (90:10%) and the values shown are based on measurements with both solvents. The numbers represent the peak numbers in decreasing mobility order. The structures of the standard compounds are presented in Figure 5 (adapted from Paper II).

Compound	Mass (u)	Ion formula	Measured ion, *m/z*	1st (K_0)	2nd (K_0)	3rd (K_0)
Pyridine	79	$[M+H]^+$	80	2.04	1.69[a]	1.63[b]
		$[M+91]^+$	170[b]	1.64		
2-*t*BPyr	135	$[M+H]^+$	136	1.73		
2,6-D*t*BPyr	191	$M^{+\bullet}$	191[b]	1.45		
		$[M+H]^+$	192	1.50	1.45[b,c]	
		$[M+O_2]^{+\bullet}$	223[b]	1.45		
2,6-D*t*B-4-MPyr	205	$M^{+\bullet}$	205[b]	1.38		
		$[M+H]^+$	206	1.42	1.38[b,c]	
		$[M+O_2]^{+\bullet}$	237[b]	1.39		
1-Naphthol	144	$M^{+\bullet}$	144	1.72		
		$[M+H]^+$	145	1.68	1.50[d]	1.32[d]
		$[M+H+10]^+$	155	1.68		
2-Naphthol	144	$M^{+\bullet}$	144	1.73		
		$[M+H]^+$	145	1.67	1.50[d]	1.32[d]
		$[M+H+10]^+$	155	1.67		

[a] dimer, [b] peaks observed clearly only in hexane:toluene (90:10%), [c] most likely ^{13}C isotope peak of the *m/z* 191 or 205 ions, and [d] minor peaks which are observed sporadically.

2,6-D*t*BPyr and 2,6-D*t*B-4-MPyr behaved similarly in the IMS analysis, and the 1st mobility peaks of their protonated molecules had higher mobilities (K_0 = 1.50 and 1.42 cm^2/Vs, respectively) than the peaks of their radical cations (K_0 = 1.45 and 1.38 cm^2/Vs, respectively, Figure 10A). Their dioxygen adducts $[M+O_2]^{+\cdot}$ had the same mobilities as the radical cations (K_0 = 1.45 and 1.39 cm^2/Vs, within experimental error, Figure 10B). The mass difference for the protonated molecules and the dioxygen adducts could explain the mobility difference.

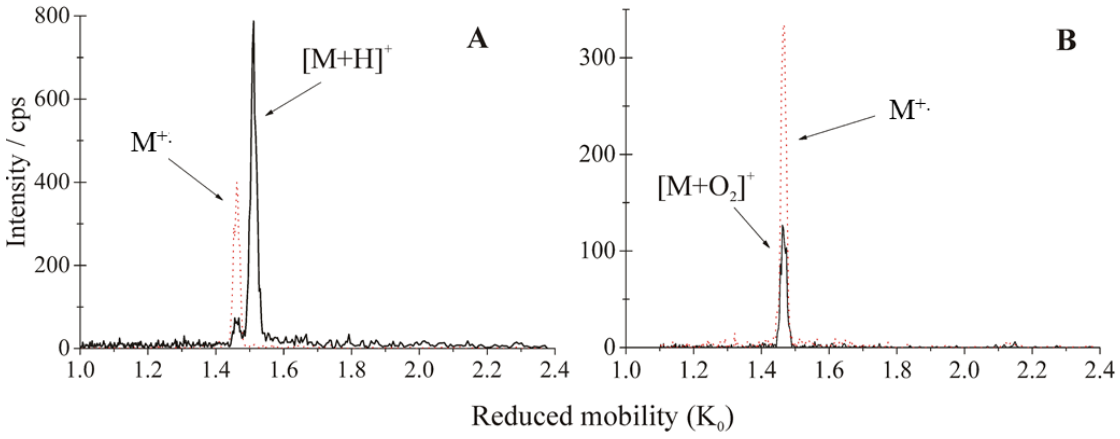

Figure 10. Positive ion APPI mass-selected mobility spectra of 2,6-D*t*BPyr dissolved in hexane:toluene (90:10%). (A) $M^{+\cdot}$ at *m/z* 191 (dotted line) and $[M+H]^+$ at *m/z* 192 (solid line). (B) $M^{+\cdot}$ (dotted line) and $[M+O_2]^{+\cdot}$ (solid line) at *m/z* 191 and *m/z* 223, respectively, shared the same mobility [127].

Interestingly, the radical cations of 1- and 2-naphthol at *m/z* 144 had higher mobilities (K_0 = 1.72 and 1.73 cm^2/Vs) than their protonated molecules at *m/z* 145 (K_0 = 1.68 and 1.68 cm^2/Vs, Table 8). However, in the case of 2,6-D*t*BPyr and 2,6-D*t*B-4-MPyr the $M^{+\cdot}$ had lower mobilities due to the formation of dioxygen adducts. This is because the $[M+H]^+$ ions of 1- and 2-naphthol interact more with the residual water in the drift gas than the $M^{+\cdot}$, as similarly reported for anilines [74]. Additional support for our results is given by Fernández-maestre *et al.* who showed that the reduced mobility of $[M+H]^+$ ion of 2,6-D*t*BPyr is independent of the water concentration in the drift gas [15].

Additional mobility measurements were done for 2,6-D*t*BPyr with an APPI-IMS-FP instrument. These measurements showed the same mobility peaks for 2,6-D*t*BPyr as in the IMS-MS measurement, as well as an reaction ion peak (RIP). Typically, a FP detector measures all the ions, and therefore also a RIP is seen. With IMS-MS, the mobilities are measured only for selected analyte ions, and therefore a RIP is not seen.

A RIP is not necessarily observed with IMS-FP instruments either, for example Borsdorf *et al.* [70, 74] does not report a RIP in his APPI-IMS studies. This could be due to different sample introduction methods and ionization conditions. Borsdorf *et al.* introduced the analytes directly into the gas phase by heating the pure analytes without dissolving them in solvents. However, in our studies the analytes were introduced to the ionization chamber along with the solvent and / or dopant.

To summarise, depending on the ionization conditions, 2,6-D*t*BPyr and 2,6-D*t*B-4-MPyr efficiently produced both radical cations $M^{+\cdot}$ and protonated $[M+H]^+$ molecules. The radical cations $M^{+\cdot}$ had longer drift times. Further analysis revealed the presence of dioxygen adduct ions $[M+O_2]^{+\cdot}$, which also had the same mobility as the radical cations $M^{+\cdot}$. Since 2-*t*BPyr does not produce the dioxygen adduct, its formation is likely to be dependent on the presence of two *tert*-butyl groups on both sides of the nitrogen "locking" the dioxygen in the middle. In cases of 1- and 2-naphthols, the radical cations $M^{+\cdot}$ had higher mobilities than the protonated molecules $[M+H]^+$, which is opposite to 2,6-D*t*BPyr and 2,6-D*t*B-4-MPyr. The $[M+O_2]^{+\cdot}$ formation of the $M^{+\cdot}$ ions of 2,6-D*t*BPyr and 2,6-D*t*B-4-MPyr increases the mass, and therefore both $M^{+\cdot}$ and $[M+O_2]^{+\cdot}$ ions have lower mobilities than the $[M+H]^+$ ions.

3.3 Separation of isomeric amines with IMS-FP (Paper III)

The aim of this study was to investigate how structural differences in isomeric compounds can affect their separation in IMS. Eight model isomeric amine standard compounds (M_r=121, $C_8H_{11}N$, Figure 6 and Table 9) were studied using positive APCI- and APPI-IMS-FP instrument. Literature reports mobility values for some of the amines used in our study, namely 4-ethylaniline [75], *N*,*N*-dimethylaniline [137, 138] and 2,4,6-collidine [138-140], but the same set of isomeric amines measured in our study was not included to the previous studies.

Mass spectrometric measurements showed that with APCI and APPI ionization techniques protonated molecules $[M+H]^+$ at *m/z* 122 were formed for all the amines. 2,6-D*t*BPyr was used as an instrumental standard and its $[M+H]^+$ ion was observed at *m/z* 192. Reduced mobilities of the analytes measured with IMS-FP and some literature values are presented in Table 9. The reproducibility of mobility experiments was

evaluated using a mobility value for the 2,6-D*t*BPyr measured with APCI (n = 8, on two different days, K_0 = 1.47 cm^2/Vs), which had a standard deviation of 0.3%.

Reduced mobility measured with APCI and APPI for 2,4,6-Col is well in line with values reported in the literature (1.82 [138, 139] and 1.84 cm^2/Vs [140]). The mobility differences of *N*,*N*-DMA between our experiments and the values reported in the literature (Table 9) could be explained by a different drift tube design, different ionization conditions, or a higher drift tube temperature (323-473 K) than that used in our experiments (296 K). Karpas et al. [137, 138] used a ^{63}Ni β ion source to produce $[M+H]^+$ ions, and they reported two different mobility peaks for *N*,*N*-DMA. They were suspected to be due to different protonation sites in the molecule, i.e., the proton could be attached to the N atom or to the ring [137]. In our experiments, we observed only one mobility peak for all the amines. In the case of 4-EA one obvious explanation for the difference in the reported mobility values is the ion measured, i.e. radical cation by Borsdorf et al. [75] and protonated molecule in our study.

Some amines had distinctly different mobility values, while others shared nearly the same mobilities (Table 9). The compound class had an important role in mobility values. For instance, compounds with a *N*-heterocyclic aromatic ring (2,4,6-Col, 1.81 cm^2/Vs), tertiary (*N*,*N*-DMA, 1.75 cm^2/Vs) or secondary amines (*N*-M-*o*-T, 1.70 cm^2/Vs) had the highest mobility values and were separated clearly. The rest of the compounds were primary amines, which had lower mobilities (Table 9, Figure 11). It is suggested that the protonated -NH_2 group (-NH_3^+) interacts more with the drift gas, and therefore the primary amines had lower mobilities, whereas in tertiary and secondary amines the protonated group is more protected from interactions with the drift gas. This is a similar "shielding" effect, where two *tert*-butyl groups of 2,6-D*t*BPyr are protecting the charge in both sides of the protonated nitrogen [12, 15]. Interestingly, PEA and 4-EA were separated (K_0 = 1.62 and 1.58 cm^2/Vs, respectively), which could be because the protonated PEA forms a "loop" via –NH_3^+ interaction with the benzene ring. Therefore, it has a "closed" shape and is likely to interact less with the drift gas than the protonated 4-EA. The side chain of 4-EA is too short to form a "loop" leaving it with the "open" shape. In the IMS literature, protonated diamines and polyamines have been reported to form also a "loop" [141].

Table 9. Summary of the reduced mobility K_0 (cm^2/Vs) values for the isomeric amines (M_r = 121) and 2,6-di-*tert*-butylpyridine (M_r = 191) measured with an IMS-FP instrument using nitrogen as the drift gas. The mobility values have not been normalized with the mobility of 2,6-D*t*BPyr. The structures of the standard compounds are presented in Figure 6 (adapted from Paper III).

Compound	**Abbreviation**	**APCI $[M+H]^+$** K_0 (cm^2/Vs)	**APPI $[M+H]^+$** K_0 (cm^2/Vs)	**Literature values** K_0 (cm^2/Vs)
2,4,6-Collidine[a]	2,4,6-Col	1.81	1.80	1.82 [138, 139], 1.84 [140], $[M+H]^+$
N,N-Dimethylaniline[a]	*N,N*-DMA	1.75	1.75	1.87 [137], 1.81 [137, 138], $[M+H]^+$
N-methyl-*o*-Toluidine[a]	*n*-M-*o*-T	1.70	1.69	
2-Phenethylamine[b]	PEA	1.62	1.62	
4-Ethylaniline[b]	4-EA	1.58	1.58	1.77 [75], $M^{+\cdot}$
2-Methylbenzylamine[c]	2-MBA	1.61	1.61	
4-Methylbenzylamine[c]	4-MBA	1.60	1.57	
3-Methylbenzylamine[c]	3-MBA	1.60	1.58	
2,6-di-*tert*-butylpyridine[d]	2,6-D*t*BPyr	1.47		

[a] Measured from Mix A; [b] Measured from Mix B; [c] Measured individually; [d] Measured from Mix B and Mix C.

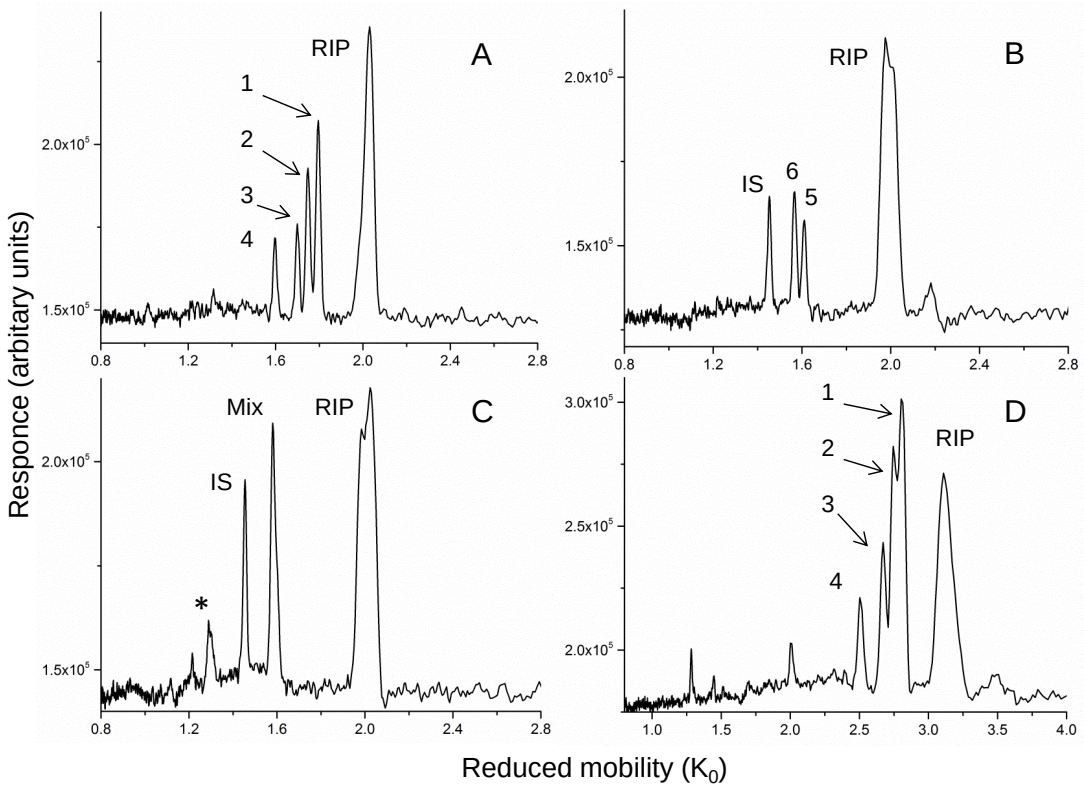

Figure 11. Positive APCI ion mobility spectra of mixtures of isomeric amines measured with IMS-Faraday plate detector (A, D) 1 = 2,4,6-Col, 2 = *N,N*-DMA, 3 = *n*-M-*o*-T and 4 = 2-MBA, (B) 5 = PEA and 6 = 4-EA, and (C) Mix = 2-, 3-, and 4-MBA. In (A, C) the drift gas was nitrogen and in (D) 33% helium and 67% nitrogen. RIP = reaction ion peak, IS = 2,6-D*t*BPyr and the asterisk (*) indicates possible amine cluster ions.

The most common drift gases are air and nitrogen. The change of the drift gas physical properties could result in better separation of the analytes that share the same mobility with nitrogen as the drift gas [142]. For example, chloroaniline and iodoaniline are not separated when nitrogen is used as drift gas, but when helium is used as drift gas they are clearly separated [142]. Therefore, in our experiments the drift gas was modified by mixing argon or helium to the nitrogen nitrogen in order to study if enhanced separation is obtained. The presence of heavier argon molecules shifted the mobilities of all the amines towards lower values, while in the presence of lighter helium molecules the mobility shifted towards higher values (Figure 12). Similar trends have been reported in the literature, where the mobility of compounds increased when helium was used as the drift gas instead of nitrogen, and decreased when argon was

used [138, 142]. However, the change of drift gas did not result in better separation of the unresolved compounds.

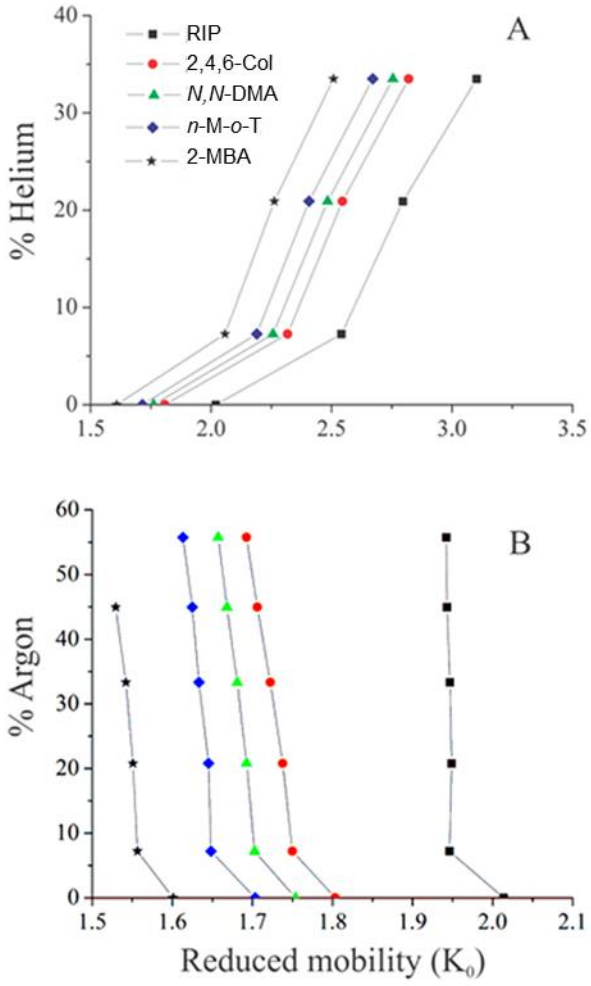

Figure 12. Reduced mobility values of isomeric amines measured with positive APCI-IMS-FP. The drift gas was nitrogen mixed with helium (A) or argon (B) (adapted from Paper III).

As a summary, the isomeric amines formed protonated molecules $[M+H]^+$ with both ionization techniques: APCI and APPI. 2,4,6-Col, *N*,*N*-DMA and *n*-M-*o*-T were separated clearly from each other with IMS, while the rest of the amines had mobility values very close to each other. However, PEA and 4-EA were separated. The major explanation for the different reduced mobilities is different shielding of the protonated nitrogen by the adjacent functional groups. In other words, the more protected the charge is e.g *N*-heterocyclic aromatic ring (2,4,6-Col) vs. primary amines, the less the

ionized analyte can interact with the drift gas, and therefore it can move faster through the drift tube.

3.4 Geochemistry of Recôncavo Basin, Brazil, oils (Paper IV)

Most of the crude oil samples from the Recôncavo Basin, Brazil, share similar biological source material and thermal maturation levels, therefore it is not easy to differentiate between them by using conventional analyzing techniques such as GC-MS. In Paper IV the differentiation of 20 oil samples from the Recôncavo Basin was made with GC×GC-TOF-MS.

The Recôncavo Basin with an area of approx. 11500 km^2 is located in Bahia, northeastern Brazil and it has started to form in the late Jurassic-early Cretaceous period [143]. Petroleum exploration of this basin, which is now in a mature stage, dates back to the 1930's. Lacustrine shales are considered to be the predominant source rock units of the basin and the main reservoirs are pre-rift sandstones [144, 145].

All the samples were measured using the GC×GC-TOF-MS instrument and the peak areas of geochemically interesting compounds were calculated from the measurement data. In addition to traditionally used geochemically interesting compounds (Paper IV), some non-conventional biomarkers were included in this study. The most significant variations in concentration between the oil samples were observed in geochemical compounds namely, β-carotane; 20S + 20R C27 5α,14α,17α-cholestanes; C_{30} 17α-diahopane; gammacerane; C_{31} 17α(H),21β(H)-homohopane; C_{30} 17α(H),21β(H)-hopane; C_{31} 3β-methylhopane; 8α(H), 14α(H)-onocerane; 8α(H), 14β(H)-onocerane; C_{24} tetracyclic terpane; and C_{26} tricyclic terpane. In total 52 geochemically interesting compounds were identified (excluding diamondoids). The peak areas of these compounds were used to calculate peak area ratios, which are typically called geochemical parameters. These parameters and their significance have been described by Peters et al. [123]. For example, in Paper IV the geochemical parameters provided information about different geochemical conditions, such as variations in biological source input material (Table 1 and 2, Paper IV) and the thermal stress conditions (Table 3 and 4, Paper IV). Biodegradation of crude oil by bacteria can also alter the geochemical parameters. This information can be used in oil exploration to distinguish between different oil samples.

Based on the plots presenting geochemical ratios of β-carotane or gammacerane / C_{30} 17α(H),21β(H)-hopane (β-car / H_{30}, Figure 13; Gam/H_{30}, Figure 14) as a function of C_{30} 17α(H),21β(H)-hopane / 20*S* + 20*R* C_{27} 5α,14α,17α-cholestanes (H_{30}/St) ratio, it was observed that the samples with high ratios of β-car/H_{30} and Gam/H_{30} were mainly located in the central area of the basin. The presence of an elevated concentration of β-carotane is associated with saline lacustrine paleoenvironments and the elevation in the concentration of gammacerane is commonly related to hypersalinity, highly specific for water-column stratification [123]. Our results (Figures 13 and 14) reveal that the salinity was not constant through time or throughout the whole ancient lake in the Recôncavo Basin.

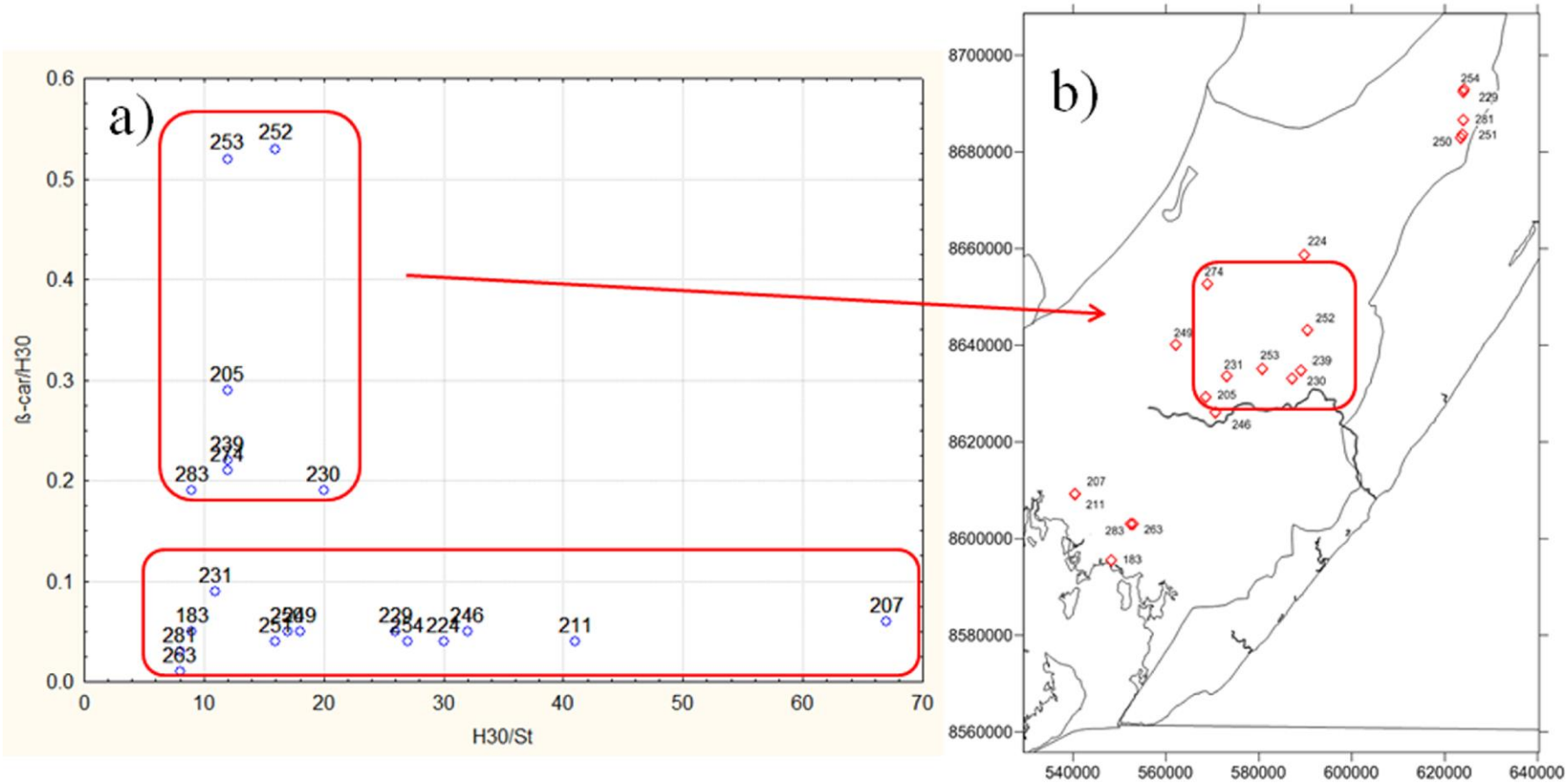

Figure 13. (A) β-carotane / C_{30} 17α(H),21β(H)-hopane (β-car/H_{30}) ratio vs. C_{30} 17α(H),21β(H)-hopane / 20*S* + 20*R* C_{27} 5α,14α,17α-cholestanes (H_{30}/St) graph, and (B) Recôncavo Basin map with samples from the central region highlighted. A larger map of the Recôncavo Basin is presented in Figure 1, Paper IV (adapted from Paper IV).

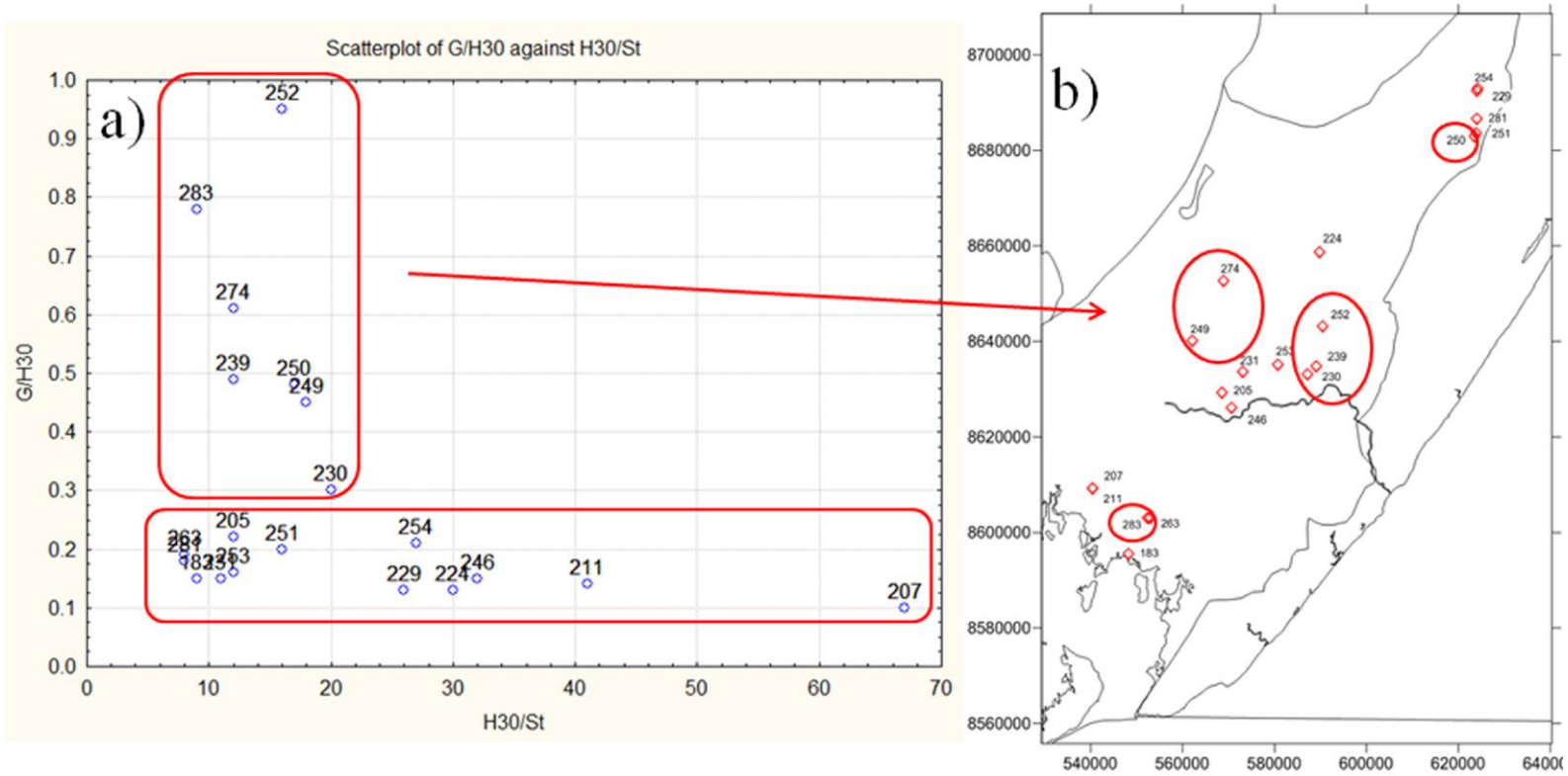

Figure 14. (A) Gammacerane / C_{30} 17α(H),21β(H)-hopane (G/H_{30}) ratio vs. C_{30} 17α(H),21β(H)-hopane / 20*S* + 20*R* C_{27} 5α,14α,17α-cholestanes (H_{30}/St) graph and (B) Recôncavo Basin map with samples from the central region highlighted. A large map of the Recôncavo Basin is presented in Figure 1, Paper IV (adapted from Paper IV).

To further simplify the large number of geochemical parameters, the statistical method, PCA was used to transform the complex results into a clear format. Figure 15 shows PCA results where principle components 1 and 2 are presented on the x and y-axis, respectively. Through this analysis only samples 253 and 274 were separated from the other samples. A further study of the results, showed that in the case of sample 253 (Figure 16A) the ratios mainly responsible for the separation, according to the score contributions, were 8α(H), 14α(H)-onocerane / C_{30} 17α(H),21β(H)-hopane (ONII/H_{30}); 8α(H), 14β(H)-onocerane / C_{30} 17α(H),21β(H)-hopane (ONIII/H_{30}); and C_{30} 17α-diahopane / C_{30} 17α(H),21β(H)-hopane (DiaH_{30}/H_{30}). Onoceranes are associated with restricted basins in warm and humid tropical climates such as Brazil [112]. Their origin is unclear, but it is thought to be related to terrigenous dominated ferns and flowering plants [123]. Diahopanes are most likely formed by oxidation and rearrangement of hopenes [146]. For sample 274, the PCA score contributions showed that the ratios of C_{31} 3β-methylhopane / C_{30} 17α(H),21β(H)-hopane (3βMH_{31}/H_{30}); C_{24} tetracyclic terpane / C_{26} tricyclic terpane (TeT_{24}/Tr_{26}); and C_{31} 17α(H),21β(H)-homohopane / C_{30} 17α(H),21β(H)-hopane ($H_{31}R$/H_{30}) mainly contributed to its separation (Figure 16B). The precursor of 3β-methylhopane is the 3β-methyl-hopanoid synthesized by several types of methanotrophic bacteria [147, 148] and the oils with 3βMH_{31}/H_{30} ratio 1% are typically from lacustrine source rocks [111]. The geochemical significance of tri– and tetracyclic terpenes are discussed in the next chapter (Geochemistry and identification of compounds in Brazilian crude oils). The high $H_{31}R$/H_{30} ratio is associated with marine and marine carbonate oils [123]. The oils 253 and 274 were distinguished from the rest of the oils mainly by non-conventional biomarker ratios.

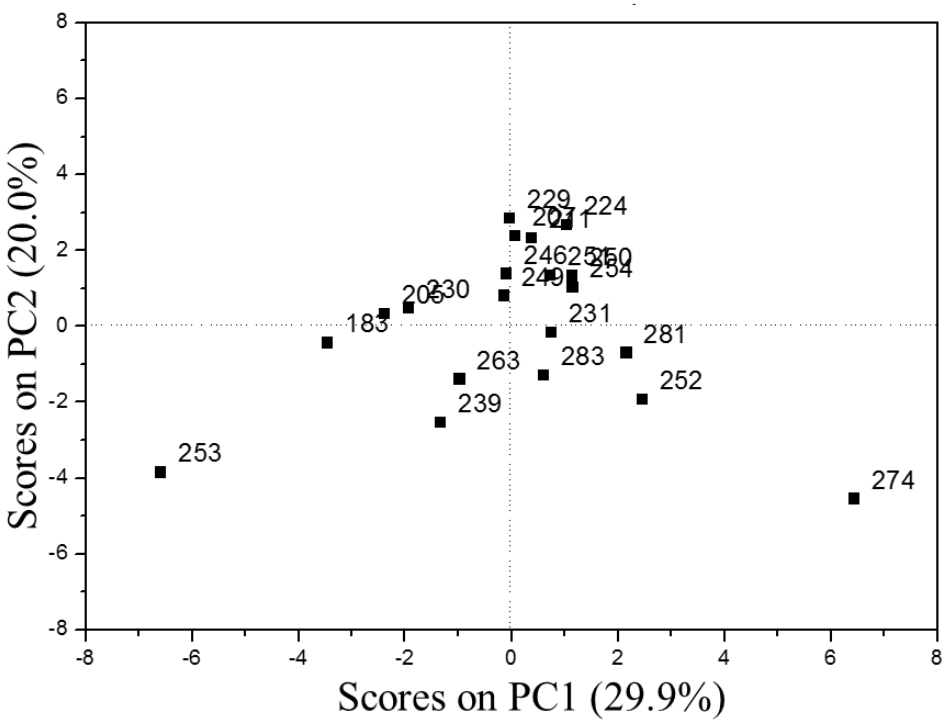

Figure 15. PCA score plots of geochemical source parameters (adapted from paper IV).

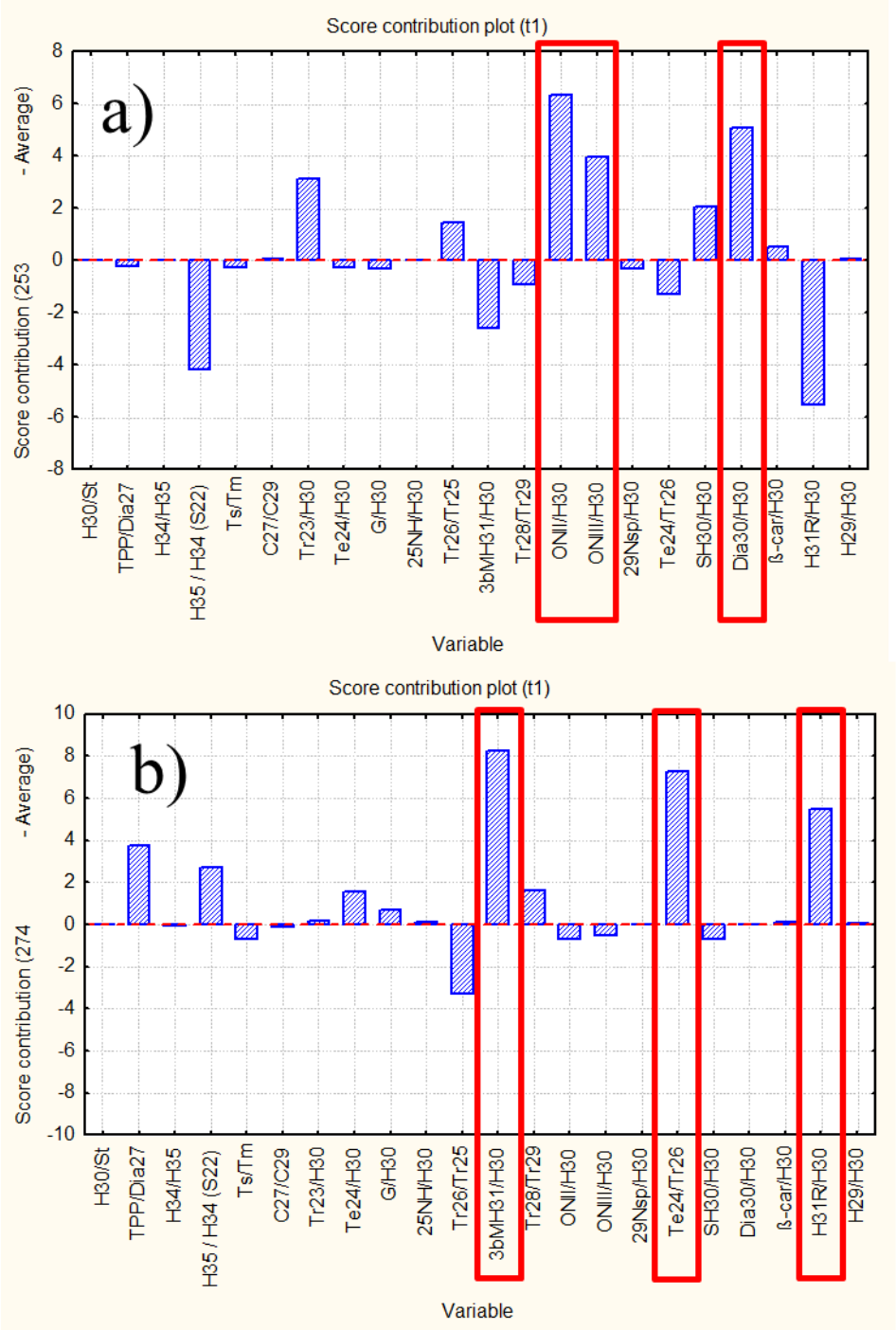

Figure 16. Parameter contributions to sample 253 (a) and 274 (b) in the PCA score plot illustrated in Figure 15. The red box illustrates biomarker ratios, which separated the sample (adapted from Paper IV).

3.5 Geochemistry and identification of compounds in Brazilian crude oils (Paper V)

In Paper V, eleven crude oil samples from different regions of Brazil, classified based on proprietary methods by the Research Center of Petrobras (CENPES) as having different source, biodegradation and maturity levels, were further analyzed with GC×GC-TOF-MS. The peak area data obtained was used for the calculation of the saturated and aromatic geochemical parameters. The saturated geochemical parameters assigned five (S01, S02, S08, S09 and S10), of the oils as originating from lacustrine source rocks, five from marine (S04, S05, S6, S07 and S11) and one (S03) as a mixture of marine and lacustrine source rocks. The 25-*nor*-hopane / C_{30} 17α(H),21β(H)-hopane (25-NH/H_{30}) ratio assigned the oils S02 and S07 as biodegraded.

The saturated and aromatic geochemical parameters obtained from GC×GC-TOF-MS were analyzed by PCA (data not shown). However, the loading plot was difficult to read due to the large quantity of parameters, therefore another PCA was done with selected geochemical source parameters. This new calculation gave a similar result as the one with the large number of geochemical parameters, but produced Figures (Figure 17) which are easier to interpret. The PCA separated most mature oils (S05, S06 and S07, Figure 17A) and the loading plots in Figure 17B illustrate that the oils were mainly separated by parameters based on aromatic compounds and saturated maturity biomarker ratios.

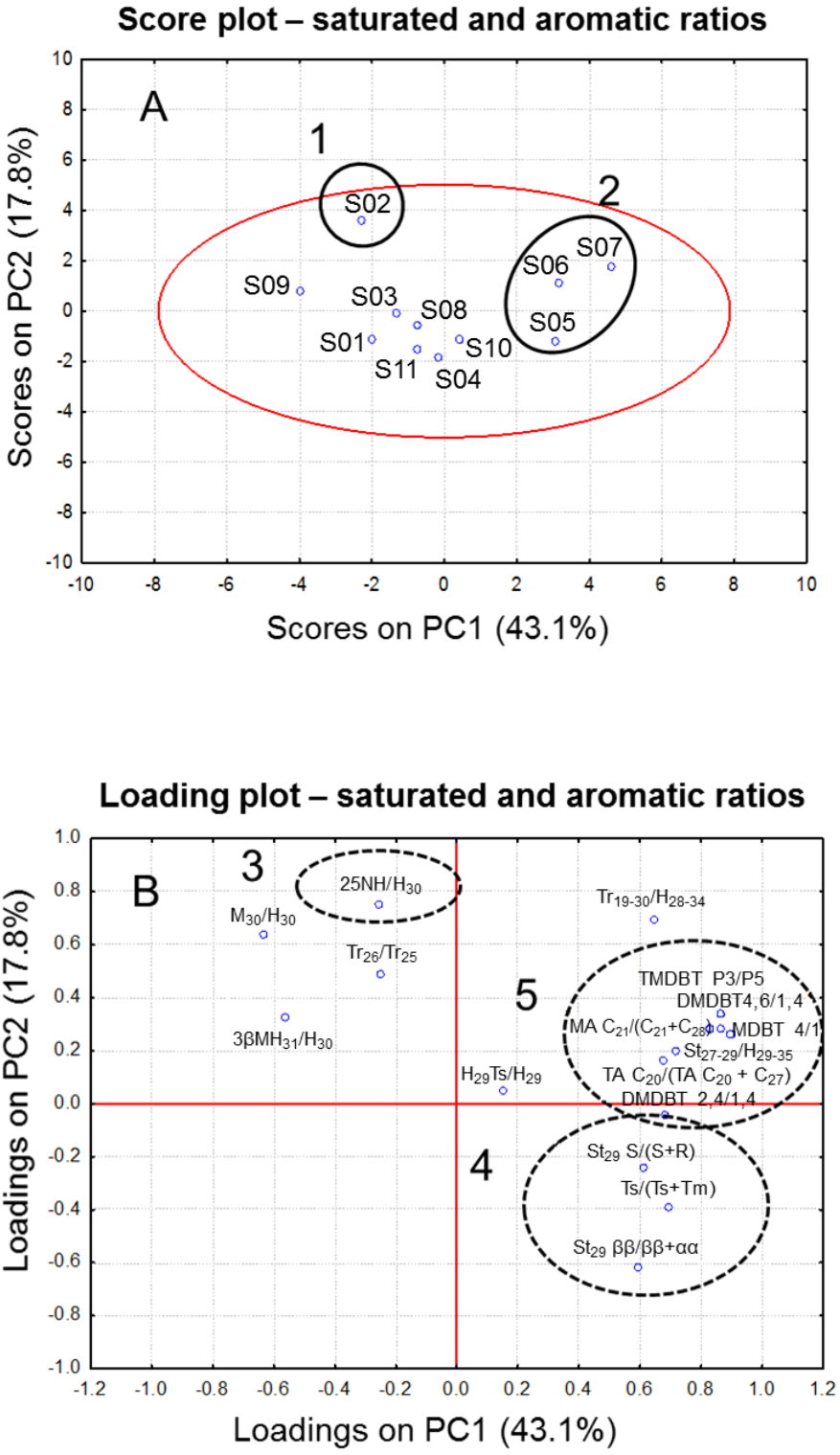

Figure 17. PCA score (A) and loading (B) plots for the first two principal components, based on saturated and aromatic biomarker parameters. [1] Oil S02; [2] Oils S05, S06 and S07; [3] 25NH/H_{30} ratio; [4] some of the saturated maturity parameters; [5] aromatic geochemical parameters.

During the data analysis, eight unknown compounds (Figure 18), not reported earlier in the literature, were observed. These compounds had the molecular ion ($M^{+\cdot}$) at *m/z* 274, 288 or 316. Two of these compounds had a common characteristic fragment at *m/z* 191 in their EI mass spectrum, and the remaining six compounds had a common fragment at *m/z* 203. All the new (or unusual) compounds were found in the B/C oil fraction meaning that they are saturated hydrocarbons, *i.e.*, these compounds contain only carbon and hydrogen atoms. Therefore, it was straightforward to calculate the double bond equivalence (DBE), or degree of unsaturation, for all these compounds from the masses of the molecular ions. The DBE formula calculates how many hydrogens are "lost" from the saturated structure. The DBE for all the compounds was four.

The new compounds had different retention times in ^{1}D and in ^{2}D GC (Figure 18 and Table 10). In the chromatographic conditions used in this study (see section 2.6) the group type separation in the ^{2}D dimension follows the order of: (i) tricyclic terpanes; (ii) steranes with 3 rings containing 6 carbon atoms and 1 ring containing 5 carbon atoms; (iii) tetracyclic terpanes with 4 rings containing 6 carbon atoms; (iv) pentacyclic terpanes with 4 rings containing 6 carbon atoms and 1 ring containing 5 carbon atoms and (v) pentacyclic terpanes with 5 rings containing 6 carbon atoms. In this group type separation, the observation that the eight new compounds are in the two dimensional separation plane somewhere between tricyclic terpanes and pentacyclic terpanes (Figure 18), and the DBE number of four, give reason to expect that the new compounds could be tetracyclic compounds.

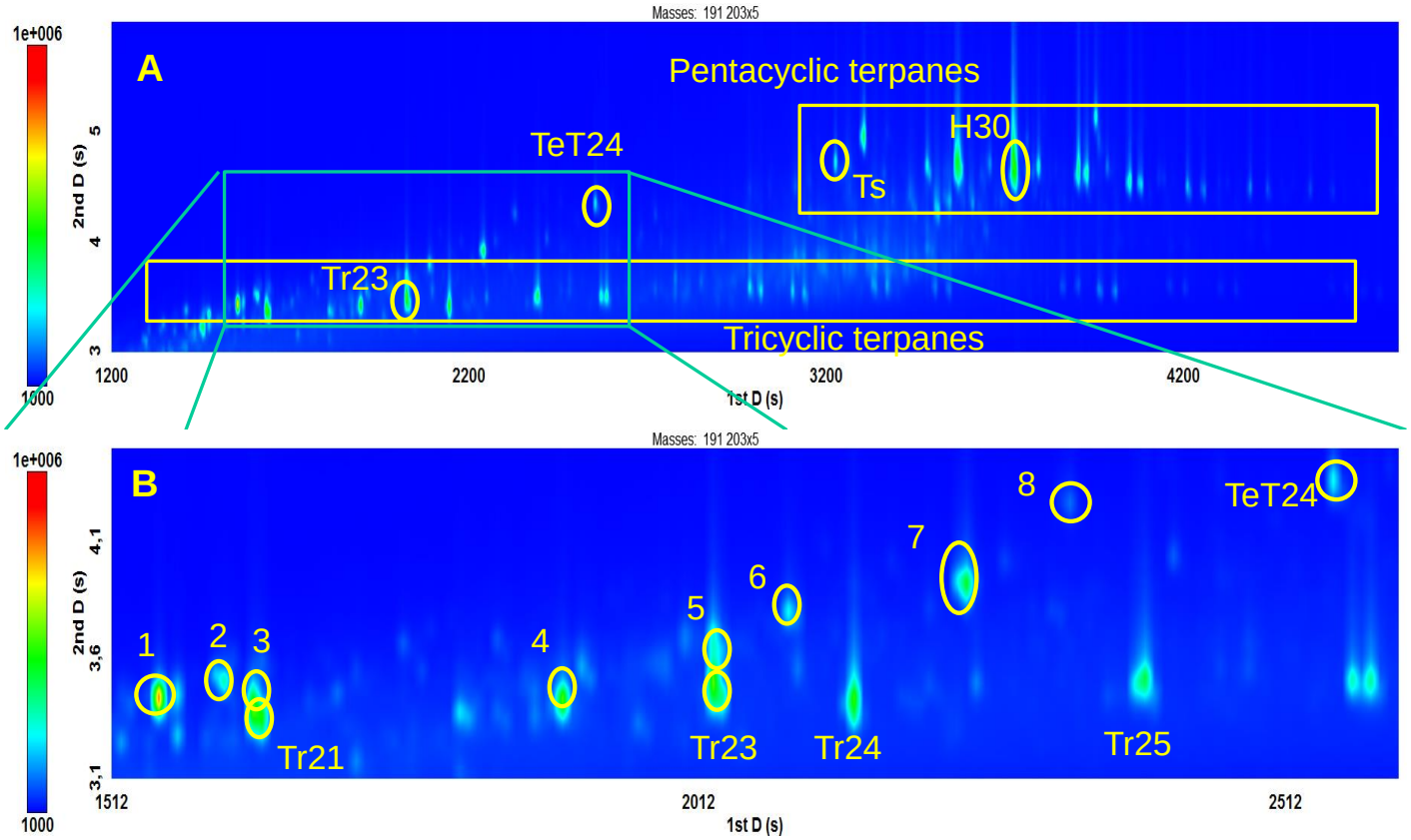

Figure 18. Crude oil sample S08: Partial extracted ion chromatogram with sums of ions at *m/z* 191 and 203 showing tri-, tetra-, and pentacyclic terpanes (A) and eight (1-8) new compounds (B). H30 = 17α(H),21β(H)-Hopane; TeT24 = C_{24} tetracyclic terpane; Tr_n = C_n tricyclic terpane; Ts = C27 18α-22,29,30-Trisnorneohopano (adapted from Paper V).

To achieve more information about the structures of the new compounds, the retention times of the compounds, for which the separation in a ^{2}D column was known, were plotted against the numerical values calculated based on the number of rings of 6 carbon atoms and number of rings of 5 carbon atoms in three reference compounds (Figure 19). The known reference compounds are C_{29} tricyclic terpane, which has three 6 carbon rings (with given ring number = 3); C_{29} 5α(H),14β(H),17β(H)-stigmastane 20R, which has three 6 carbon rings and one 5 carbon ring (with given ring number = 3.5) and C_{29} 17α(H),21β(H)hopane, which has four 6 carbon rings and one 5 carbon ring (with given ring number = 4.5) (see Figure 19 for structures). The ring numbers (Table 10) for the eight new compounds were assigned according to the best fit line obtained based on the known biomarker retention times. The ring numbers for the eight new compounds varied in the range from 2.86 to 3.91, representing approximately those of from tricyclic (3.00) to tetracyclic terpanes (4.00).

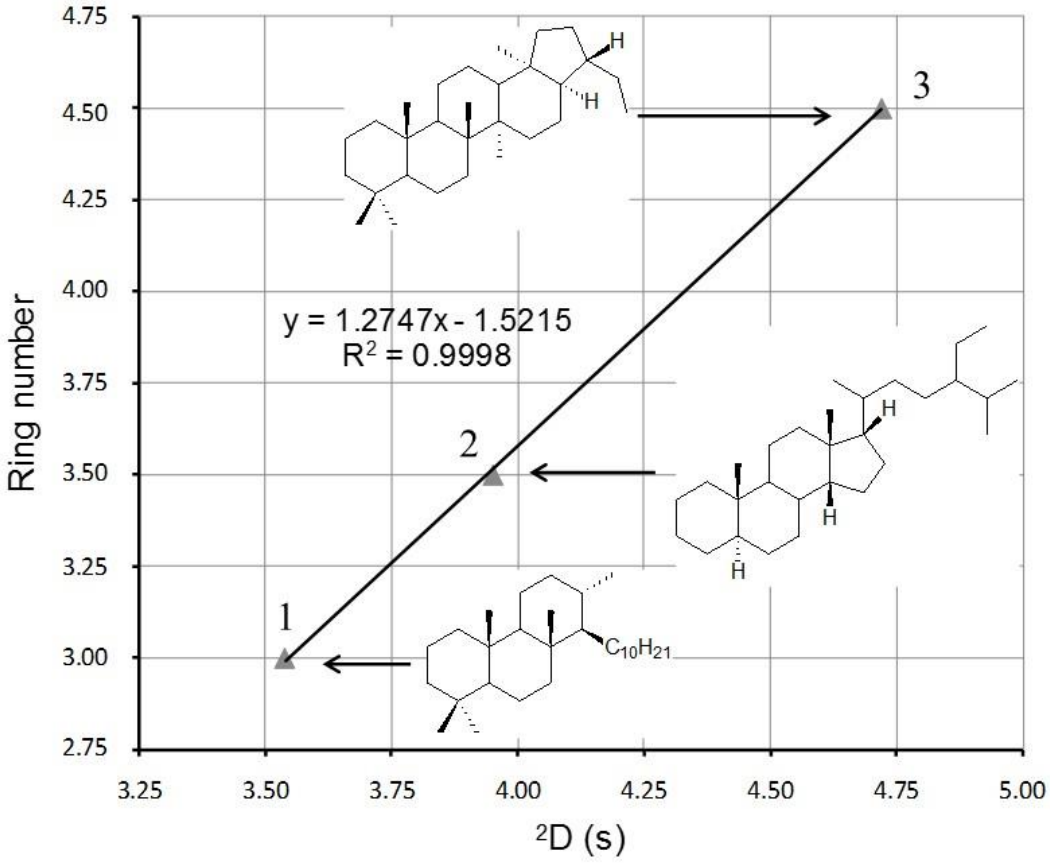

Figure 19. ^{2}D retention time vs. ring number curve of (1) C_{29} tricyclic terpane, (2) C_{29} 5α(H),14β(H),17β(H)-stigmastane 20R and (3) C_{29} 17α(H),21β(H)hopane, which were used to calculate the ring number values in Table 10 (adapted from Paper V).

Table 10. Retention times (t_R) in ^{1}D (t_1) and ^{2}D (t_2), and ring numbers for selected known biomarkers, as well as the calculated ring numbers for new tetracyclic compounds (Figure 19), which are marked with bold font. The numbers represent the new tetracyclic compounds observed in the chromatogram in Figure 18.

Name	MM	t_{R1} (s)	t_{R2} (s)	Carbons	Ring number
C_{20} tricyclic terpane	276	1448	3.24	20	3.00[b]
C_{21} tricyclic terpane	290	1632	3.40	21	3.00[b]
C_{24} tricyclic terpane	332	2144	3.43	24	3.00[b]
C_{24} tetracyclic terpane	330	2552	4.36	24	4.00[b]
C_{27} 13β(H),17α(H)-diacholestane 20R	372	2848	3.65	27	3.50[b]
C_{27} 5α(H),14β(H),17β(H)-stigmastane 20R	372	3112	3.89	27	3.50[b]
C_{27} 22,29,30-trisnorneohopane (Ts)	370	3224	4.73	27	4.50[b]
C_{27} 22,29,30-trisnorhopane (Tm)	370	3304	4.93	27	4.50[b]
C_{29} tricyclic terpane	402	3136	3.54	29	3.00[b]
C_{29} 5α(H),14β(H),17β(H)-stigmastane 20R	400	3480	3.95	29	3.50[b]
C_{29} Hopane	398	3568	4.72	29	4.50[b]
Gammacerane	412	3952	5.14	30	5.00[b]
8α,14α Onocerane II	414	3576	3.83	30	2+2[b]
#1, $C_{20}H_{34}$	274	1552	3.44	20	2.86[a]
#2, $C_{20}H_{34}$	288	1608	3.63	21	3.11[a]
#3, $C_{21}H_{36}$	288	1640	3.61	21	3.08[a]
#4, $C_{23}H_{40}$	316	1896	3.44	23	2.86[a]
#5, $C_{23}H_{40}$	316	2024	3.72	23	3.22[a]
#6, $C_{23}H_{40}$	316	2088	3.81	23	3.34[a]
#7, $C_{23}H_{40}$	316	2240	3.93	23	3.49[a]
#8, $C_{23}H_{40}$	316	2328	4.26	23	3.91[a]

[a] The calculated ring number based on a linear trend line equation presented in Figure 19.
[b] Given number according to the number of carbon rings in the molecule; a five-carbon ring reduces the number by 0.5.

Exact matches for the MS spectra of compounds 1-8 (Figure 20) were not found in the literature (Table 4, Paper V), therefore the structural identification, including ring configurations is relying on the compounds´ retention times and MS fragmentation.

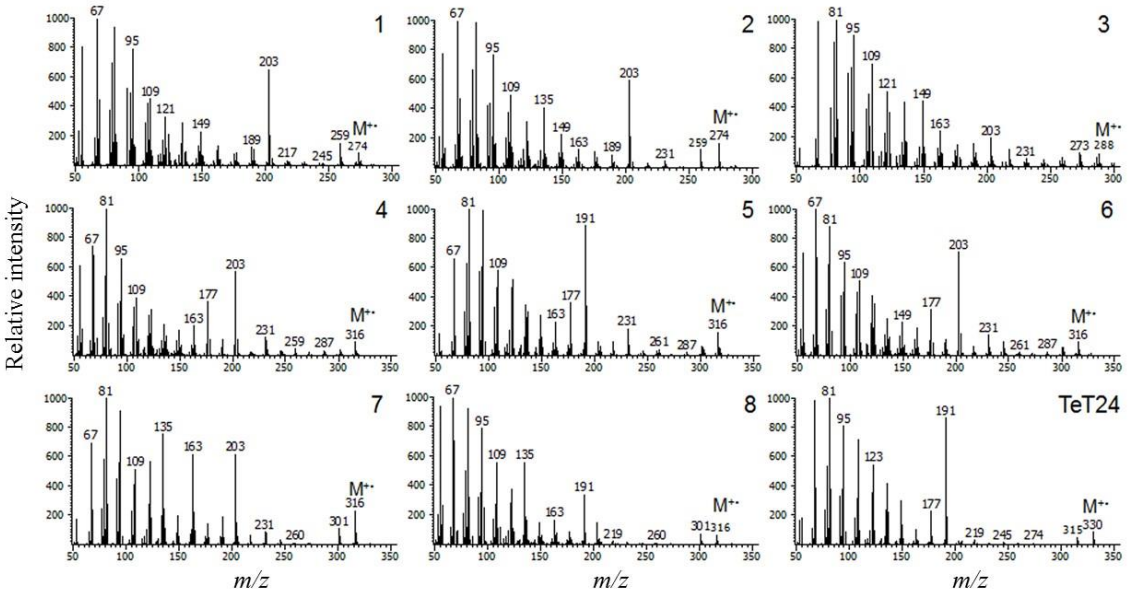

Figure 20. EI mass spectra of new compounds (1-8) and C_{24} tetracyclic terpane (TeT24) (adapted from Paper V).

Even when the measurements are conducted with a two dimensional gas chromatography obtaining "clean" EI mass spectra is not easy. This is demonstrated in Figure 21. The compound 4 co-eluted with another compound also in ^{2}D, resulting in a single peak in TIC (marked with an asterisk in Figure 21). Careful spectral examination and software assisted deconvolution resulted in clear MS spectra for C_{23} tricyclic terpane (A, Figure 21) and compound 4 (B, Figure 20 and 21). The detection of this compound with conventional GC-MS would be very difficult, as in the detection of minor differences of oils in section 3.4. For example, 3βMH_{31} can not always be detected with GC-MS, because it elutes close to H_{31R} and Gam [111].

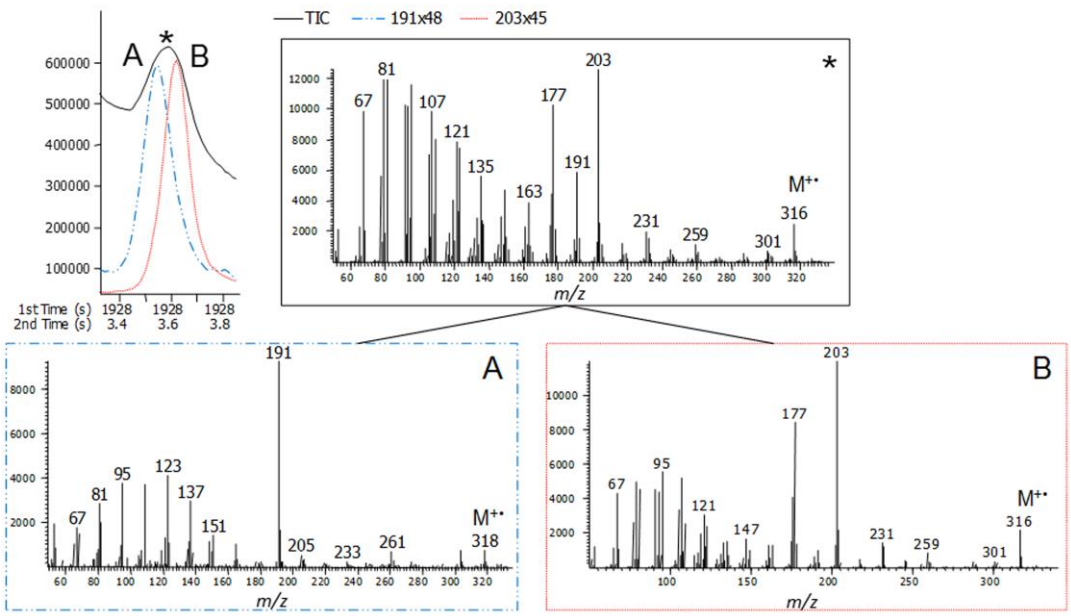

Figure 21. Top left: Total ion chromatogram (TIC) (*, black solid line); extracted ion chromatogram at *m/z* 191 (A, blue dashed line, peak intensity x48), and extracted ion chromatogram at *m/z* 203 (B, red solid line, peak intensity x45). Top right: mass spectrum at the top of the TIC peak. Bottom left: Mass spectrum of co-eluting possible C_{23} tricyclic terpane with diagnostic ion *m/z* 191 (A) taken at the top of the blue dashed line. Bottom right: New C_{23} tetracyclic compound (Compound 4, Figure 18B and 21) with diagnostic ion *m/z* 203 (B) taken at the top of the red solid line (adapted from Paper V).

The chromatographic and MS information for the new compounds were combined and the most likely tentative structures for compounds 1, 3, 4 and 8 are proposed (Figure 22). For instance, compound 4 has retention time close to tricyclic terpanes and it has a 4 ring structure. Therefore it could be possible to have a of the ring C, which could cause a reduction in retention time in ^{2}D. Compounds 6 and 7 have similar MS spectra to compound 4, but a higher retention times in ^{2}D, which indicate a different ring structure. Compound 8 has a retention time in ^{2}D close to the C_{24} tetracyclic terpane and a fragment ion at *m/z* 191. This ion is typical to C_{24} tetracyclic terpane [150], and therefore compound 8 could be a C_{23} tetracyclic terpane. Compound 2 could have a similar structure as compound 1, because their retention times in ^{2}D are similar and in MS spectrum they have similar fragment ions. The MS spectrum of compound 5 is close to compound 8, and therefore compound 5 could have a partially similar structure. To summarise, all the new compounds are assumed to have a tetracyclic saturated structure.

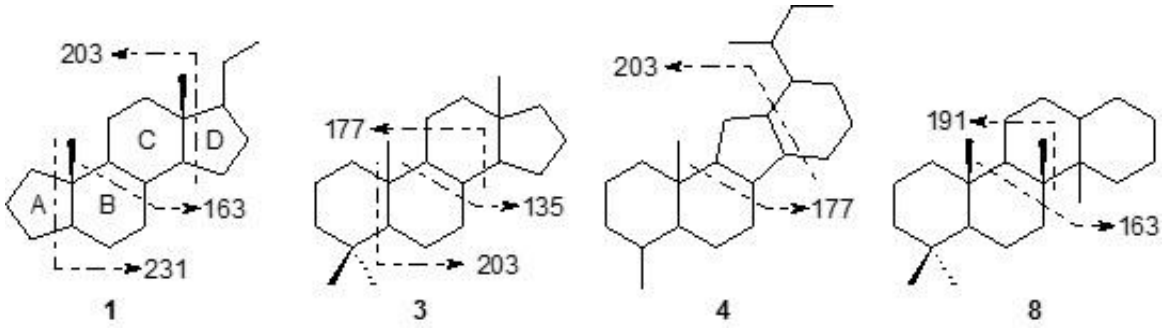

Figure 22. Tentative structures and possible fragmentations for new biomarkers (1, 3, 4 and 8) in Figure 18 (adapted from Paper V).

The new tetracyclic compounds were encountered with varying concentrations in all 11 crude oil samples collected from different regions of Brazil.

The peak areas of the new tetracyclic compounds were divided with the peak area of C_{24} tetracyclic terpane (A_c/TeT24, Supplementary material, Table 2S, Paper V). The new ratios were analyzed with PCA together with already known saturated and aromatic geochemical parameters as presented in Figure 17. The loading plot results showed that A_c/TeT24 ratios acted in the same direction as dibenzothiophene ratios, which indicates that some of the new compounds could respond to changes in maturation in a similar way as dibenzothiophenes. Similar results were observed in score plots when the ratios of compound 7/TeT_{24} and compound 8/TeT_{24} were plotted with the ratio of dimethyldibenzothiophene (DMDBT) 4,6/1,4. The samples S06 and S07, which both showed high ratios of compound 7/TeT_{24} and 8/TeT_{24} when the ratio of DMDBT 4,6/1,4 was high.

A more detailed score plot (data not shown) examination of the samples revealed a correlation between the peak areas of compound 7 and TeT24, which could mean that compound 7 is formed from TeT24 during the maturation process, or the compounds could have a common precursor. Therefore, it is proposed that the ratios of compound 7 / TeT24 could be used as potential new maturity parameter, for more mature oils, similar to benzothiophenes, which have been used for oils in the maturity window for vitrinite reflectance R_0 ~1.3-1.5 (Chakhmakhchev et al., 1997). Nevertheless, the maturation working range of these tetracyclic compounds should be determined in more detail.

4. CONCLUSIONS

Two different pre-separation techniques, IMS (Papers I-III) and GC×GC (IV-V) combined with MS, were studied in this thesis. Their capacity in difficult analytical tasks was demonstrated by separating model isomeric compounds with IMS and by oil analysis with GC×GC-TOF-MS.

Paper I studied the behavior of selected phenolic compounds and 2,4,6-TNT using negative APCI-IMS-MS. 2-*t*BPh formed two ion species $[M-H]^-$ and $[M-H+O]^-$, interestingly; the heavier $[M-H+O]^-$ ion had a shorter drift time than the lighter $[M-H]^-$ ion. This could be due to the fact that the $[M-H]^-$ ion forms an adduct, for example with NO_x or O_x, which is separated from analyte after IMS separation and is not detected with MS. The increased mass of an adduct ion $[M-H+?]^-$ could result in a longer drift time than $[M-H+O]^-$ ion, or the interaction with the drift gas is different for these two ion species. Where $[M-H]^-$ ion is more prone to interactions than $[M-H+O]^-$, which could form an internal hydrogen bond resulting in the charge being more protected. Three compounds, 2,6-D*t*BPh, 2,6-D*t*B-4-MPh and 2,4,6-T*t*BPh, behaved similarly in the different IMS measuring conditions used in this study, producing two mobility peaks for the $[M-H]^-$ ion, which are not dependent on the measuring conditions used. Therefore, it can be suggested that these three phenolic compounds could be used as mobility standards in addition to 2,4,6-TNT, but further characterization is required. In addition, two isomeric compounds 2,4-D*t*BPh and 2,6-D*t*BPh were clearly separated with IMS.

Paper II demonstrated that in correct APPI ionization conditions, 2,6-D*t*BPyr and 2,6-D*t*B-4-MPyr efficiently produce both radical cations $M^{+\cdot}$ and protonated $[M+H]^+$ molecules. Also, dioxygen adduct ions $[M+O_2]^{+\cdot}$, which had the same mobility as $M^{+\cdot}$, were observed. Therefore, it can be proposed that the $M^{+\cdot}$ ions are formed together with $[M+O_2]^{+\cdot}$ ions. The lower mobility of $[M+O_2]^{+\cdot}$ ions than of $[M+H]^+$, can be explained by the mass difference, i.e., heavier ions have longer drift times than lighter ions. The dioxygen adduct formation is likely to depend on the presence of two *tert*-butyl groups on both sides of the nitrogen "locking" the dioxygen in the middle. The naphthols produced both $M^{+\cdot}$ and $[M+H]^+$ ions. Interestingly, the $M^{+\cdot}$ ions had higher mobilities than the $[M+H]^+$ ions, which is opposite to 2,6-D*t*BPyr and 2,6-D*t*B-4-MPyr, for which also oxygen adducts were formed. The mobility order of different naphthol ions could

be due to different locations of the charge, for example the $[M+H]^+$ ion could be protonated in the -OH group, whereas in the $M^{+\cdot}$ ion the charge could be delocalized in the benzene rings. This could result in different conformation of molecules with different collision cross-sections of ion species.

In Paper III, both APCI and APPI produced protonated molecules $[M+H]^+$ for isomeric amines. Clear separation was recorded for 2,4,6-colidine, *N*,*N*-dimethylaniline, *N*-methyl-*o*-toluidine, phenethylamine and 4-ethylaniline with IMS, while the rest of the amines had mobility values very close to each other. This can be explained by the structures of isomers. For instance, the shielded molecules, i.e., with a protected charge (e.g. 2,4,6-collidine), interact less with the drift gas than the molecules with more open structures, such as primary amines.

In Paper IV, crude oil analysis from Recôncavo Basin was carried out with GC×GC-TOF-MS. Important geochemical parameters were calculated based on the GC×GC-TOF-MS results and evaluated. The PCA of the geochemical parameters was able to separate two oils from a total of twenty oils. The geochemical parameters also indicated that β-carotane can be used to reconstruct salinity variations in the late Jurassic to early Cretaceous time in an ancient lake during the fragmentation of the Pangaea supercontinent.

In Paper V, the source and maturity-related geochemical parameters were measured for eleven Brazilian crude oils using GC×GC-TOF-MS. A relationship between the retention time in ^{2}D and the carbon ring structure was observed for several biomarkers already known from the literature. Since all the analyte compounds were saturated hydrocarbons (their polarity did not vary significantly), it is assumed that the shape of the molecule has an important role in the interactions with the column surface. The data about a relationship between the retention time in ^{2}D and the carbon ring was used to achieve more structural information about eight new compounds found during the analysis. Using mass spectral data to calculate the DBE and the information from retention time in ^{2}D, it could be suggested that these new compounds had tetracyclic structures, some of them similar to nor-steranes. It was also observed that compound 7/TeT24 ratio increases together with the DMDBT 4,6/1,4 ratio. This could be due to the fact that the compound 7 is more stable than the C_{24} tetracyclic terpane or it is produced during the maturation process. The compound 7/TeT24 ratio could be used in the future, in parallel with other maturation indicators such as benzothiophenes (R_0

~1.3-1.5) to evaluate oils from mature to overmature levels. Still, the maturity range for these new tetracyclic compounds should be characterized in more detail.

IMS is a faster measuring technique (typical analysis time is ~1 sec) with smaller peak capacity ~10^2 (total number of theoretical plates) [151] than GC×GC, which has peak capacity >$2*10^4$ [90] with slower analysis time (typical analysis time is ~1 h). In IMS and GC×GC the separation of coeluting compounds can be improved in some cases by optimizing the measuring conditions, such as the polarity of the drift gas in IMS or the polarity of the columns in GC×GC. Furthermore, in IMS, ionized compounds are separated in a drift region and in GC×GC, the neutral molecules are separated. The shape of the molecule can change during the ionization process therefore these two techniques complement each other. IMS can be miniaturized for field analysis, while GC×GC instruments are typically benchtop size for laboratory use.

Both IMS and GC×GC, are capable of separating isomers. In IMS the most important property for separation of isomeric compounds is their shape (collision cross section). In addition to this, it was shown that different isomers have differing tendencies to form adducts. For example, in the negative APCI mode the formation of dioxygen adduct was seen for 2,4-D*t*BPh but not for 2,6-D*t*BPh. The dioxygen adduct of 2,4-D*t*BPh increased the mass of the ion resulting in a slower drift time than for the lighter [M-H]+ ion of 2,6-D*t*BPh. This basic finding could be adapted in different fields of chemistry to increase the understanding of the fundamental behavior of regio isomers. For example, isomers have a significant role in complex biological processes. Adducts (e.g. dioxygen) are well known in IMS and MS literature, but commonly they are dissociated in MS interface with declustering voltage or with curtain gas. Reactive oxygen species, such as hydrogen peroxide or peroxynitrite, are part of the production of dioxygen radical ions in living cells. It could be possible that dioxygen adducts are formed with molecules, which have similar structure than model compounds in this work, in real biological process. In the future, it would be interesting to study these adducts.

REFERENCES

1. Watson, J.T., Sparkman, O.D.: Introduction to Mass Spectrometry. John Wiley & Sons, Ltd. p. 862 (2008)
2. Hamilton, R.J.: Introduction to high performance liquid chromatography. In: Hamilton R.J., Sewell P.A. (eds.). Springer Netherlands, p. 248 (1982)
3. James, A.T., Martin, A.J.P.: Gas-liquid partition chromatography: the separation and micro-estimation of volatile fatty acids from formic acid to dodecanoic acid. Biochemical Journal. **50**, 679-690 (1952)
4. Eiceman, G.A., Karpas, Z., Hill, H.H.: Ion Mobility Spectrometry, 3rd ed., CRC Press Taylor & Francis, Boca Raton. p. 444 (2013)
5. Adahchour, M., Beens, J., Vreuls, R.J.J., Brinkman, U.A.T.: Recent developments in comprehensive two-dimensional gas chromatography (GCxGC): I. Introduction and instrumental set-up. Trends in Analytical Chemistry. **25**, 438-454 (2006)
6. Adahchour, M., Beens, J., Vreuls, R.J.J., Brinkman, U.A.T.: Recent developments in comprehensive two-dimensional gas chromatography (GCxGC): II. Modulation and detection. Trends in Analytical Chemistry. **25**, 540-553 (2006)
7. Adahchour, M., Beens, J., Vreuls, R.J.J., Brinkman, U.A.T.: Recent developments in comprehensive two-dimensional gas chromatography (GCxGC): III. Applications for petrochemicals and organohalogens. Trends in Analytical Chemistry, **25**, 726-741 (2006)
8. Bertsch, W.: Two-Dimensional Gas Chromatography. Concepts, Instrumentation, and Applications – Part 1: Fundamentals, Conventional Two-Dimensional Gas Chromatography, Selected Applications. Journal of High Resolution Chromatography. **22**, 647-665 (1999)
9. Marriott, P.J., Chin, S.-T., Maikhunthod, B., Schmarr, H.-G., Bieri, S.: Multidimensional gas chromatography. Trends in Analytical Chemistry. **34**, 1-21 (2012)
10. Mason, E.A.: Plasma Chromatography, Plenum, New York. p. 259 (1984)
11. Viidanoja, J., Sysoev, A., Adamov, A., Kotiaho, T.: Tetraalkylammonium halides as chemical standards for positive electrospray ionization with ion mobility spectrometry/mass spectrometry. Rapid Communications in Mass Spectrometry. **19**, 3051-3055 (2005)
12. Eiceman, G.A., Nazarov, E.G., Stone, J.A.: Chemical standards in ion mobility spectrometry. Analytica Chimica Acta. **493**, 185-194 (2003)
13. Kaur-Atwal, G., O'Connor, G., Aksenov, A., Bocos-Bintintan, V., Paul Thomas, C.L., Creaser, C.: Chemical standards for ion mobility spectrometry: a review. International Journal for Ion Mobility Spectrometry. **12**, 1-14 (2009)
14. Viitanen, A.K., Mauriala, T., Mattila, T., Adamov, A., Pedersen, C.S., Mäkelä, J.M., Marjamäki, M., Sysoev, A., Keskinen, J., Kotiaho, T.: Adjusting mobility scales of ion mobility spectrometers using 2,6-D*t*BP as a reference compound. Talanta. **76**, 1218-1223 (2008)
15. Fernandez-Maestre, R., Harden, C.S., Ewing, R.G., Crawford, C.L., Hill, H.H.: Chemical standards in ion mobility spectrometry. Analyst. **135**, 1433-1442 (2010)
16. Thomas, C.L.P., Rezgui, N.D., Kanu, A.B., Munro, W.A.: Measuring the temperature of the drift gas in an ion mobility spectrometer: a technical note. International Journal for Ion Mobility Spectrometry. **5**, 31-36 (2002)

17. Crawford, C.L., Hauck, B.C., Tufariello, J.A., Harden, C.S., McHugh, V., Siems, W.F., Hill, H.H.: Accurate and reproducible ion mobility measurements for chemical standard evaluation. Talanta. **101**, 161-170 (2012)
18. Kanu, A.B., Hill Jr, H.H.: Identity confirmation of drugs and explosives in ion mobility spectrometry using a secondary drift gas. Talanta. **73**, 692-699 (2007)
19. Spangler, G.E., Collins, C.I.: Reactant ions in negative ion plasma chromatography. Analytical Chemistry. **47**, 393-402 (1975)
20. Kanu, A.B., Dwivedi, P., Tam, M., Matz, L., Hill, H.H.: Ion mobility–mass spectrometry. Journal of Mass Spectrometry. **43**, 1-22 (2008)
21. Clemmer, D.E., Jarrold, M.F.: Ion Mobility Measurements and their Applications to Clusters and Biomolecules. Journal of Mass Spectrometry. **32**, 577-592 (1997)
22. Wittmer, D., Chen, Y.H., Luckenbill, B.K., Hill, H.H.: Electrospray Ionization Ion Mobility Spectrometry. Analytical Chemistry. **66**, 2348-2355 (1994)
23. Bothner, B., Siuzdak, G.: Electrospray Ionization of a Whole Virus: Analyzing Mass, Structure, and Viability. ChemBioChem. **5**, 258-260 (2004)
24. Borsdorf, H., Schelhorn, H., Flachowsky, J., Döring, H.-R., Stach, J.: Corona discharge ion mobility spectrometry of aliphatic and aromatic hydrocarbons. Analytica Chimica Acta. **403**, 235-242 (2000)
25. Pedersen, C.S., Lauritsen, F.R., Sysoev, A., Viitanen, A.-K., Mäkelä, J.M., Adamov, A., Laakia, J., Mauriala, T., Kotiaho, T.: Characterization of Proton-Bound Acetate Dimers in Ion Mobility Spectrometry. Journal of the American Society for Mass Spectrometry. **19**, 1361-1366 (2008)
26. Borsdorf, H., Nazarov, E.G., Miller, R.A.: Time-of-flight ion mobility spectrometry and differential mobility spectrometry: A comparative study of their efficiency in the analysis of halogenated compounds. Talanta. **71**, 1804-1812 (2007)
27. Sielemann, S., Baumbach, J.I., Schmidt, H., Pilzecker, P.: Detection of alcohols using UV-ion mobility spetrometers. Analytica Chimica Acta. **431**, 293-301 (2001)
28. Menéndez, M., Garrido-Delgado, R., Arce, L., Valcárcel, M.: Direct determination of volatile analytes from solid samples by UV-ion mobility spectrometry. Journal of Chromatography A. **1215**, 8-14 (2008)
29. Adamov, A., Mauriala, T., Teplov, V., Laakia, J., Pedersen, C.S., Kotiaho, T., Sysoev, A.A.: Characterization of a high resolution drift tube ion mobility spectrometer with a multi-ion source platform. International Journal of Mass Spectrometry. **298**, 24-29 (2010)
30. Rahel, J., Pavlik, M., Holubcik, L., Sobek, V., Skalny, J.D.: Relaxing Phenomena in Negative Corona Discharge: New Aspects. Contributions to Plasma Physics. **39**, 501-513 (1999)
31. Crawford, C.L., Hill, H.H.: Comparison of reactant and analyte ions for ^{63}Nickel, corona discharge, and secondary electrospray ionization sources with ion mobility-mass spectrometry. Talanta. **107**, 225-232 (2013)
32. Skalny, J.D., Orszagh, J., Mason, N.J., Rees, J.A., Aranda-Gonzalvo, Y., Whitmore, T.D.: Mass spectrometric study of negative ions extracted from point to plane negative corona discharge in ambient air at atmospheric pressure. International Journal of Mass Spectrometry. **272**, 12-21 (2008)

33. Waltman, M.J., Dwivedi, P., Hill Jr, H.H., Blanchard, W.C., Ewing, R.G.: Characterization of a distributed plasma ionization source (DPIS) for ion mobility spectrometry and mass spectrometry. Talanta. **77**, 249-255 (2008)
34. Ross, S.K., Bell, A.J.: Reverse flow continuous corona discharge ionisation applied to ion mobility spectrometry. International Journal of Mass Spectrometry. **218**, L1-L6 (2002)
35. Kauppila, T.J., Kostiainen, R., Bruins, A.P.: Anisole, a new dopant for atmospheric pressure photoionization mass spectrometry of low proton affinity, low ionization energy compounds. Rapid Communications in Mass Spectrometry. **18**, 808-815 (2004)
36. Kauppila, T.J., Kuuranne, T., Meurer, E.C., Eberlin, M.N., Kotiaho, T., Kostiainen, R.: Atmospheric Pressure Photoionization Mass Spectrometry. Ionization Mechanism and the Effect of Solvent on the Ionization of Naphthalenes. Analytical Chemistry. **74**, 5470-5479 (2002)
37. Kauppila, T.J., Kotiaho, T., Kostiainen, R., Bruins, A.P.: Negative ion-atmospheric pressure photoionization-mass spectrometry. Journal of the American Society for Mass Spectrometry. **15**, 203-211 (2004)
38. Kolakowski, B.M., Mester, Z.: Review of applications of high-field asymmetric waveform ion mobility spectrometry (FAIMS) and differential mobility spectrometry (DMS). Analyst. **132**, 842-864 (2007)
39. Tang, F., Wang, X., Xu, C.: FAIMS Biochemical Sensor Based on MEMS Technology, New Perspectives in Biosensors Technology and Applications, Prof. Pier Andrea Serra (Ed.), ISBN: 978-953-307-448-1, InTech, Available from: http://www.intechopen.com/books/new-perspectives-in-biosensorstechnology-and-applications/faims-biochemical-sensor-based-on-mems-technology. (2011)
40. Shvartsburg, A.A.: Differential Ion Mobility Spectrometry. CRC Press, p. 322 (2008)
41. Giles, K., Pringle, S.D., Worthington, K.R., Little, D., Wildgoose, J.L., Bateman, R.H.: Applications of a travelling wave-based radio-frequency-only stacked ring ion guide. Rapid Communications in Mass Spectrometry. **18**, 2401-2414 (2004)
42. Pringle, S.D., Giles, K., Wildgoose, J.L., Williams, J.P., Slade, S.E., Thalassinos, K., Batemana, R.H., Bowersc, M.T., Scrivens, J.H.: An investigation of the mobility separation of some peptide and protein ions using a new hybrid quadrupole/travelling wave IMS/oa-ToF instrument. International Journal of Mass Spectrometry. **261**, 1-12 (2007)
43. Castellanos, A., Benigni, P., Hernandez, D.R., DeBord, J.D., Ridgeway, M.E., Park, M.A., Fernandez-Lima, F.: Fast screening of polycyclic aromatic hydrocarbons using trapped ion mobility spectrometry-mass spectrometry. Analytical Methods. **6**, 9328-9332 (2014)
44. Sysoev, A., Adamov, A., Viidanoja, J., Ketola, R.A., Kostiainen, R., Kotiaho, T.: Development of an ion mobility spectrometer for use in an atmospheric pressure ionization ion mobility spectrometer/mass spectrometer instrument for fast screening analysis. Rapid Communications in Mass Spectrometry. **18**, 3131-3139 (2004)
45. Xia, Y.-Q., Wu, S.T., Jemal, M.: LC-FAIMS-MS/MS for Quantification of a Peptide in Plasma and Evaluation of FAIMS Global Selectivity from Plasma Components. Analytical Chemistry. **80**, 7137-7143 (2008)

46. Myung, S., Lee, Y.J., Moon, M.H., Taraszka, J., Sowell, R., Koeniger, S., Hilderbrand, A.E., Valentine, S.J., Cherbas, L., Cherbas, P., Kaufmann, T.C., Miller, D.F., Mechref, Y., Novotny, M.V., Ewing, M.A., Sporleder, R.C., Clemmer, D.E.: Development of High-Sensitivity Ion Trap Ion Mobility Spectrometry Time-of-Flight Techniques: A High-Throughput Nano-LC-IMS-TOF Separation of Peptides Arising from a Drosophila Protein Extract. Analytical Chemistry. **75**, 5137-5145 (2003)
47. Henderson, S.C., Valentine, S.J., Counterman, A.E., Clemmer, D.E.: ESI/Ion Trap/Ion Mobility/Time-of-Flight Mass Spectrometry for Rapid and Sensitive Analysis of Biomolecular Mixtures. Analytical Chemistry. **71**, 291-301 (1999)
48. Ruotolo, B.T., Gillig, K.J., Stone, E.G., Russell, D.H., Fuhrer, K., Gonin, M., Schultz, J.A.: Analysis of protein mixtures by matrix-assisted laser desorption ionization-ion mobility-orthogonal-time-of-flight mass spectrometry. International Journal of Mass Spectrometry. **219**, 253-267 (2002)
49. Valentine, S.J., Plasencia, M.D., Liu, X., Krishnan, M., Naylor, S., Udseth, H.R., Smith, R.D., Clemmer D.E.: Toward Plasma Proteome Profiling with Ion Mobility-Mass Spectrometry. Journal of Proteome Research. **5**, 2977-2984 (2006)
50. Ewing, R.G., Atkinson, D.A., Eiceman, G.A., Ewing, G.J.: A critical review of ion mobility spectrometry for the detection of explosives and explosive related compounds. Talanta. **54**, 515-529 (2001)
51. Lee, J., Park, S., Cho, S.G., Goh, E.M., Lee, S., Koh, S.-S., Kim, J.: Analysis of explosives using corona discharge ionization combined with ion mobility spectrometry–mass spectrometry. Talanta. **120**, 64-70 (2014)
52. Sabo, M., Malásková, M., Matejčík, Š.: Ion mobility spectrometry–mass spectrometry studies of ion processes in air at atmospheric pressure and their application to thermal desorption of 2,4,6-trinitrotoluene. Plasma Sources Science and Technology. **23**, 015025 (2014)
53. Armenta, S., Alcala, M., Blanco, M.: A review of recent, unconventional applications of ion mobility spectrometry (IMS). Analytica Chimica Acta. **703**, 114-123 (2011)
54. Ewing, M.A., Glover, M.S., Clemmer, D.E.: Hybrid ion mobility and mass spectrometry as a separation tool. Journal of Chromatography A. **1439**, 3-25 (2016)
55. Wu, C., Hill, H.H., Rasulev, U.K., Nazarov, E.G.: Surface Ionization Ion Mobility Spectrometry. Analytical Chemistry. **71**, 273-278 (1999)
56. Tuovinen, K., Kolehmainen, M., Paakkanen, H.: Determination and identification of pesticides from liquid matrices using ion mobility spectrometry. Analytica Chimica Acta. **429**, 257-268 (2001)
57. Kotiaho, T., Lauritsen, F.R., Degn, H., Paakkanen, H.: Membrane inlet ion mobility spectrometry for on-line measurement of ethanol in beer and in yeast fermentation. Analytica Chimica Acta. **309**, 317-325 (1995)
58. Vautz, W., Zimmermann, D., Hartmann, M., Baumbach, J.I., Nolte, J., Jung, J.: Ion mobility spectrometry for food quality and safety. Food Additives & Contaminants. **23**, 1064-1073 (2006)
59. Strachan, N.J.C., Nicholson, F.J., Ogden, I.D.: An automated sampling system using ion mobility spectrometry for the rapid detection of bacteria. Analytica Chimica Acta. **313**, 63-67 (1995)

60. Fenn, L., Kliman, M., Mahsut, A., Zhao, S., McLean, J.: Characterizing ion mobility-mass spectrometry conformation space for the analysis of complex biological samples. Anal Bioanal Chem. **394**, 235-244 (2009)
61. Snyder, A.P., Harden, C.S., Brittain, A.H., Kim, M.G., Arnold, N.S., Meuzelaar, H.L.C.: Portable hand-held gas chromatography/ion mobility spectrometry device. Analytical Chemistry. **65**, 299-306 (1993)
62. Dwivedi, P., Wu, P., Klopsch, S., Puzon, G., Xun, L., Hill, H., Jr.: Metabolic profiling by ion mobility mass spectrometry (IMMS). Metabolomics. **4**, 63-80 (2008)
63. Dwivedi, P., Schultz, A.J., Jr, H.H.H.: Metabolic profiling of human blood by high-resolution ion mobility mass spectrometry (IM-MS). International Journal of Mass Spectrometry. **298**, 78-90 (2010)
64. Taraszka, J.A., Counterman, A.E., Clemmer, D.E.: Gas-phase separations of complex tryptic peptide mixtures. Fresenius Journal of Analytical Chemistry. **369**, 234-245 (2001)
65. Jin, L., Barran, P.E., Deakin, J.A., Lyon, M., Uhrin, D.: Conformation of glycosaminoglycans by ion mobility mass spectrometry and molecular modelling. Physical Chemistry Chemical Physics. **7**, 3464-3471 (2005)
66. McLean, J.A., Ruotolo, B.T., Gillig, K.J., Russell, D.H.: Ion mobility–mass spectrometry: a new paradigm for proteomics. International Journal of Mass Spectrometry. **240**, 301-315 (2005)
67. Fasciotti, M., Lalli, P.M., Klitzke, C.F., Corilo, Y.E., Pudenzi, M.A., Pereira, R.C.L., Bastos, W., Daroda, R.J., Eberlin; M.N.: Petroleomics by Traveling Wave Ion Mobility–Mass Spectrometry Using CO_2 as a Drift Gas. Energy & Fuels. **27**, 7277-7286 (2013)
68. Santos, J.M., Galaverna, R.d.S., Pudenzi, M.A., Schmidt, E.M., Sanders, N.L., Kurulugama, R.T., et al.: Petroleomics by ion mobility mass spectrometry: resolution and characterization of contaminants and additives in crude oils and petrofuels. Analytical Methods. **7**, 4450-4463 (2015)
69. Ahmed, A., Cho, Y., Giles, K., Riches, E., Lee, J.W., Kim, H.I., Choi, C.H., Kim, S.: Elucidating Molecular Structures of Nonalkylated and Short-Chain Alkyl ($n < 5$, $(CH_2)_n$) Aromatic Compounds in Crude Oils by a Combination of Ion Mobility and Ultrahigh-Resolution Mass Spectrometries and Theoretical Collisional Cross-Section Calculations. Analytical Chemistry. **86**, 3300-3307 (2014)
70. Ponthus, J., Riches, E.: Evaluating the multiple benefits offered by ion mobility-mass spectrometry in oil and petroleum analysis. International Journal for Ion Mobility Spectrometry. **16**, 95-103 (2013)
71. Borsdorf, H., Rudolph, M.: Gas-phase ion mobility studies of constitutional isomeric hydrocarbons using different ionization techniques. International Journal of Mass Spectrometry. **208**, 67-72 (2001)
72. Borsdorf, H.: Influence of structural features of isomeric hydrocarbons on ion formation at atmospheric pressure. International Journal for Ion Mobility Spectrometry. **11**, 27-33 (2008)
73. Borsdorf, H., Nazarov, E.G., Eiceman, G.A.: Atmospheric pressure ionization and gas phase ion mobility studies of isomeric dihalogenated benzenes using different ionization techniques. International Journal of Mass Spectrometry. **232**, 117-126 (2004)

74. Borsdorf, H., Stone, J.A., Eiceman, G.A.: Gas phase studies on terpenes by ion mobility spectrometry using different atmospheric pressure chemical ionization techniques. International Journal of Mass Spectrometry. **246**, 19-28 (2005)
75. Borsdorf, H., Neitsch, K., Eiceman, G.A., Stone, J.A.: A comparison of the ion chemistry for mono-substituted toluenes and anilines by three methods of atmospheric pressure ionization with ion mobility spectrometry. Talanta. **78**, 1464-1475 (2009)
76. Dwivedi, P., Bendiak, B., Clowers, B.H., Hill Jr, H.H.: Rapid Resolution of Carbohydrate Isomers by Electrospray Ionization Ambient Pressure Ion Mobility Spectrometry-Time-of-Flight Mass Spectrometry (ESI-APIMS-TOFMS). Journal of the American Society for Mass Spectrometry. **18**, 1163-1175 (2007)
77. Counterman, A.E., Clemmer, D.E.: Cis−Trans Signatures of Proline-Containing Tryptic Peptides in the Gas Phase. Analytical Chemistry. **74**, 1946-1951 (2002)
78. Wu, C., Siems, W.F., Klasmeier, J., Hill, H.H.: Separation of Isomeric Peptides Using Electrospray Ionization/High-Resolution Ion Mobility Spectrometry. Analytical Chemistry. **72**, 391-395 (2000)
79. Clowers, B.H., Dwivedi, P., Steiner, W.E., Hill Jr, H.H., Bendiak, B.: Separation of Sodiated Isobaric Disaccharides and Trisaccharides Using Electrospray Ionization-Atmospheric Pressure Ion Mobility-Time of Flight Mass Spectrometry. Journal of the American Society for Mass Spectrometry. **16**, 660-669 (2005)
80. Clowers, B.H., Hill, H.H.: Influence of cation adduction on the separation characteristics of flavonoid diglycoside isomers using dual gate-ion mobility-quadrupole ion trap mass spectrometry. Journal of Mass Spectrometry. **41**, 339-351 (2006)
81. Karas, M.: Separation of Components of an Analysis Sample in an Ion Mobility Spectrometer using a Supply of Selectively Interactive Gaseous Particles. US Patent. 0178340 A1 and US7015462 B2 (2004)
82. Dwivedi, P., Wu, C., Matz, L.M., Clowers, B.H., Siems, W.F., Hill, H.H.: Gas-Phase Chiral Separations by Ion Mobility Spectrometry. Analytical Chemistry. **78**, 8200-8206 (2006)
83. Benassi, M., Corilo, Y.E., Uria, D., Augusti, R., Eberlin, M.N.: Recognition and Resolution of Isomeric Alkyl Anilines by Mass Spectrometry. Journal of the American Society for Mass Spectrometry. **20**, 269-277 (2009)
84. Schenauer, M.R., Leary, J.A.: An ion mobility–mass spectrometry investigation of monocyte chemoattractant protein-1. International Journal of Mass Spectrometry. **287**, 70-76 (2009)
85. Ahonen, L., Fasciotti, M., Gennäs, G.B.a., Kotiaho, T., Daroda, R.J., Eberlin, M., Kostiainen, R.: Separation of steroid isomers by ion mobility mass spectrometry. Journal of Chromatography A. **1310**, 133-137 (2013)
86. Borsdorf, H., Nazarov, E.G., Miller, R.A.: Atmospheric-pressure ionization studies and field dependence of ion mobilities of isomeric hydrocarbons using a miniature differential mobility spectrometer. Analytica Chimica Acta. **575**, 76-88 (2006)
87. Gabryelski, W., Froese, K.L.: Rapid and sensitive differentiation of anomers, linkage, and position isomers of disaccharides using High-Field Asymmetric Waveform Ion Mobility Spectrometry (FAIMS). Journal of the American Society for Mass Spectrometry. **14**, 265-277 (2003)

88. Barnett, D.A., Purves, R.W., Ells, B., Guevremont, R.: Separation of *o*-, *m*- and *p*-phthalic acids by high-field asymmetric waveform ion mobility spectrometry (FAIMS) using mixed carrier gases. Journal of Mass Spectrometry. **35**, 976-980 (2000)
89. Lalli, P.M., Iglesias, B.A., Toma, H.E., de Sa, G.F., Daroda, R.J., Silva Filho, J.C., Szulejko, J.E., Araki, K., Eberlin, M.N.,: Protomers: formation, separation and characterization via travelling wave ion mobility mass spectrometry. Journal of Mass Spectrometry. **47**, 712-719 (2012)
90. Dimandja, J.-M.D.: Peer Reviewed: GC X GC. Analytical Chemistry. **76**, 167 A-174 A (2004)
91. Meinert, C., Meierhenrich, U.J.: A New Dimension in Separation Science: Comprehensive Two-Dimensional Gas Chromatography. Angewandte Chemie International Edition. **51**, 10460-10470 (2012)
92. NIST: The National Institute of Standards and Technology (http://chemdata.nist.gov/).
93. Pani, O., Górecki, T.: Comprehensive two-dimensional gas chromatography (GC×GC) in environmental analysis and monitoring. Anal Bioanal Chem. **386**, 1013-1023 (2006)
94. Herrero, M., Ibáñez, E., Cifuentes, A., Bernal, J.: Multidimensional chromatography in food analysis. Journal of Chromatography A. **1216**, 7110-7129 (2009)
95. Koek, M., van der Kloet, F., Kleemann, R., Kooistra, T., Verheij, E., Hankemeier, T.: Semi-automated non-target processing in GC × GC–MS metabolomics analysis: applicability for biomedical studies. Metabolomics. **7**, 1-14 (2011)
96. Hagan, S., Dunn, W.B., Knowles, J.D., Broadhurst, D., Williams, R., Ashworth, J.J., Cameron, M., Kelly, D.B.: Closed-Loop, Multiobjective Optimization of Two-Dimensional Gas Chromatography/Mass Spectrometry for Serum Metabolomics. Analytical Chemistry. **79**, 464-476 (2007)
97. Ventura, G.T., Kenig, F., Reddy, C.M., Schieber, J., Frysinger, G.S., Nelson, R.K., Dinel, E., Gaines, R.B., Schaeffer, P.: Molecular evidence of Late Archean archaea and the presence of a subsurface hydrothermal biosphere. Proceedings of the National Academy of Sciences. **104**, 14260-14265 (2007)
98. Frysinger, G.S., Gaines, R.B., Xu, L., Reddy, C.M.: Resolving the Unresolved Complex Mixture in Petroleum-Contaminated Sediments. Environmental Science & Technology. **37**, 1653-1662 (2003)
99. Song, S.M., Marriott, P., Wynne, P.: Comprehensive two-dimensional gas chromatography—quadrupole mass spectrometric analysis of drugs. Journal of Chromatography A. **1058**, 223-232 (2004)
100. Mitrevski, B., S., Wilairat, P., Marriott, P., J.: Evaluation of World Anti-Doping Agency criteria for anabolic agent analysis by using comprehensive two-dimensional gas chromatography–mass spectrometry. Analytical and Bioanalytical Chemistry. **396**, 2503-2511 (2010)
101. Eiserbeck, C., Nelson, R.K., Grice, K., Curiale, J., Reddy, C.M.: Comparison of GC-MS, GC-MRM-MS, and GCxGC to characterise higher plant biomarkers in Tertiary oils and rock extracts. Geochimica et Cosmochimica Acta. **87**, 299-322 (2012)
102. Silva, R.S.F., Tamanqueira, J.B., Dias, J.C.M., Passarelli, F.M., Bidart, A.M.F., Aquino Neto, F.R., Azevedo, D.A.: Comprehensive two-dimensional gas

chromatography with time of flight mass spectrometry applied to analysis of Fischer-Tropsch synthesis products obtained with and without carbon dioxide addition to feed gas. Journal of the Brazilian Chemical Society. **22**, 2121-2126 (2011)
103. Ávila, B.M.F., Aguiar, A., Gomes, A.O., Azevedo, D.A.: Characterization of extra heavy gas oil biomarkers using comprehensive two-dimensional gas chromatography coupled to time-of-flight mass spectrometry. Advances in Organic Geochemistry 2009 Proceedings of the 24th International Meeting on Organic Geochemistry. **41**, 863-866 (2010)
104. Ávila, B.M.F., Pereira, R., Gomes, A.O., Azevedo, D.A.: Chemical characterization of aromatic compounds in extra heavy gas oil by comprehensive two-dimensional gas chromatography coupled to time-of-flight mass spectrometry. Selected Papers from the 34th ISCC and the 7th GCxGC Symposium 34th International Symposium on Capillary Chromatography and 7th GCxGC Symposium. **1218**, 3208-3216 (2011)
105. Dutriez, T., Courtiade, M., Thiébaut, D., Dulot, H., Borras, J., Bertoncini, F., Hennion, M.-C.,: Advances in Quantitative Analysis of Heavy Petroleum Fractions by Liquid Chromatography-High-Temperature Comprehensive Two-Dimensional Gas Chromatography: Breakthrough for Conversion Processes. Energy & Fuels. **24**, 4430-4438 (2010)
106. Mahé, L., Courtiade, M., Dartiguelongue, C., Ponthus, J., Souchon, V., Thiébaut, D.: Overcoming the high-temperature two-dimensional gas chromatography limits to elute heavy compounds. Journal of Chromatography A. **1229**, 298-301 (2012)
107. Aguiar, A., Aguiar, H.G.M., Azevedo, D.A., Aquino Neto, F.R.: Identification of Methylhopane and Methylmoretane Series in Ceará Basin Oils, Brazil, Using Comprehensive Two-Dimensional Gas Chromatography Coupled to Time-of-Flight Mass Spectrometry. Energy & Fuels. **25**, 1060-1065 (2011)
108. Aguiar, A., Silva Júnior, A.I., Azevedo, D.A., Aquino Neto, F.R.: Application of comprehensive two-dimensional gas chromatography coupled to time-of-flight mass spectrometry to biomarker characterization in Brazilian oils. Fuel. **89**, 2760-2768 (2010)
109. Soares, R.F., Pereira, R., Silva, R.S.F., Mogollon, L., Azevedo, D.A.: Comprehensive two-dimensional gas chromatography coupled to time of flight mass spectrometry: new biomarker parameter proposition for the characterization of biodegraded oil. Journal of the Brazilian Chemical Society. **24**, 1570-1581 (2013)
110. Li, S., Cao, J., Hu, S., Zhang, D., Fan, R.: Analysis of terpanes in biodegraded oils from China using comprehensive two-dimensional gas chromatography with time-of-flight mass spectrometry. Fuel. **133**, 153-162 (2014)
111. Kiepper, A.P., Casilli, A., Azevedo, D.A.: Depositional paleoenvironment of Brazilian crude oils from unusual biomarkers revealed using comprehensive two dimensional gas chromatography coupled to time of flight mass spectrometry. Organic Geochemistry. **70**, 62-75 (2014)
112. Oliveira, C.R., Ferreira, A.A., Oliveira, C.J.F., Azevedo, D.A., Santos Neto, E.V., Aquino Neto, F.R.: Biomarkers in crude oil revealed by comprehensive two-dimensional gas chromatography time-of-flight mass spectrometry: Depositional paleoenvironment proxies. Organic Geochemistry. **46**, 154-164 (2012)

113. Oliveira, C.R., Oliveira, C.J.F., Ferreira, A.A., Azevedo, D.A., Aquino Neto, F.R.: Characterization of aromatic steroids and hopanoids in marine and lacustrine crude oils using comprehensive two dimensional gas chromatography coupled to time-of-flight mass spectrometry (GCxGC-TOFMS). Organic Geochemistry. **53**, 131-136 (2012)
114. Silva, R.C., Silva, R.S.F., de Castro, E.V.R., Peters, K.E., Azevedo, D.A.: Extended diamondoid assessment in crude oil using comprehensive two-dimensional gas chromatography coupled to time-of-flight mass spectrometry. Fuel. **112**, 125-133 (2013)
115. Bertoncini, F., Vendeuvre, C., Thiébaut, D.: Interest and Applications of Multidimensional Gas Chromatography for Trace Analysis in the Petroleum Industry Oil & Gas Science and Technology - Rev. IFP. **60**, 937-950 (2005)
116. Bruckner, C.A., Prazen, B.J., Synovec, R.E.: Comprehensive Two-Dimensional High-Speed Gas Chromatography with Chemometric Analysis. Analytical Chemistry. **70**, 2796-2804 (1998)
117. Frysinger, G.S., Gaines, R.B.: Comprehensive Two-Dimensional Gas Chromatography with Mass Spectrometric Detection (GC × GC/MS) Applied to the Analysis of Petroleum. Journal of High Resolution Chromatography. **22**, 251-255 (1999)
118. Hua, R., Li, Y., Liu, W., Zheng, J., Wei, H., Wang, J., Lua, X., Konga, H., Xu, G.: Determination of sulfur-containing compounds in diesel oils by comprehensive two-dimensional gas chromatography with a sulfur chemiluminescence detector. First International Symposium on Comprehensive Multidimensional Gas Chromatography. **1019**, 101-109 (2003)
119. Marshall, A.G., Hendrickson, C.L., Jackson, G.S.: Fourier transform ion cyclotron resonance mass spectrometry: A primer. Mass Spectrometry Reviews. **17**, 1-35 (1998)
120. Marshall, A.G., Rodgers, R.P.: Petroleomics: The Next Grand Challenge for Chemical Analysis. Accounts of Chemical Research. **37**, 53-59 (2004)
121. Vaz, B.G., Silva, R.C., Klitzke, C.F., Simas, R.C., Lopes Nascimento, H.D., Pereira, R.C.L., Garcia, D.F., Eberlin, M.N., Azevedo, D.A.: Assessing Biodegradation in the Llanos Orientales Crude Oils by Electrospray Ionization Ultrahigh Resolution and Accuracy Fourier Transform Mass Spectrometry and Chemometric Analysis. Energy & Fuels. **27**, 1277-1284 (2013)
122. Hughey, C.A., Rodgers, R.P., Marshall, A.G., Walters, C.C., Qian, K., Mankiewicz, P.: Acidic and neutral polar NSO compounds in Smackover oils of different thermal maturity revealed by electrospray high field Fourier transform ion cyclotron resonance mass spectrometry. Organic Geochemistry. **35**, 863-880 (2004)
123. Peters, K.E., Walters, C.C., Moldowan, J.M.: The Biomarker Guide: Biomarkers in the environment and human history, Vol 1. **2nd**, p. 471 (2005)
124. Peters, K.E., Walters, C.C., Moldowan, J.M.: The Biomarker Guide, Biomarkers and Isotopes in Petroleum Exploration and Earth History, Vol 2. **2nd**, p. 684 (2005)
125. Eiserbeck, C., Nelson, R.K., Grice, K., Curiale, J., Reddy, C.M., Raiteri, P.: Separation of 18α(H)-, 18β(H)-oleanane and lupane by comprehensive two-dimensional gas chromatography. Journal of Chromatography A. **1218**, 5549-5553 (2011)

126. Ventura, G.T., Kenig, F., Reddy, C.M., Frysinger, G.S., Nelson, R.K., Mooy, B.V., et al.: Analysis of unresolved complex mixtures of hydrocarbons extracted from Late Archean sediments by comprehensive two-dimensional gas chromatography (GC×GC). Organic Geochemistry. **39**, 846-867 (2008)
127. Laakia, J.: Applications of ion mobility spectrometry - mass spectrometry using negative atmospheric pressure chemical ionization on selected phenols, and positive atmospheric pressure photoionization for the separation of different ion structures, Ph.Lic. Thesis. University of Helsinki. (2010)
128. Marotta, E., Aquino Neto, F.R., Azevedo, D.A.: Separation and quantitative determination of linear and cyclic/branched alkanes in Brazilian petroleum using urea adduction and gas chromatography: a case study revisited. Química Nova. **37**, 1692-1698 (2014)
129. Nwadinigwe, C.A., Nwobodo, I.O.: Analysis of *n*-paraffins in light crudes: Molecular sieve and urea adduction techniques revisited. Fuel. **73**, 779-782 (1994)
130. Laakia, J., Pedersen, C.S., Adamov, A., Viidanoja, J., Sysoev, A., Kotiaho, T.: Sterically hindered phenols in negative ion mobility spectrometry-mass spectrometry. Rapid Communications in Mass Spectrometry. **23**, 3069-3076 (2009)
131. Silva, R.S.F., Aguiar, H.G.M., Rangel, M.D., Azevedo, D.A., Aquino Neto, F.R.: Comprehensive two-dimensional gas chromatography with time of flight mass spectrometry applied to biomarker analysis of oils from Colombia. Fuel. **90**, 2694-2699 (2011)
132. Cody, R.B., Laramee, J.A.: Atmospheric pressure ion source cross reference to related application. US Patent, WO 10/732205, 2004. (2005)
133. Sabo, M., Michalczuk, B., Lichvanová, Z., Kavický, V., Radjenovic, B., Matejčík, Š.: Interactions of multiple reactant ions with 2,4,6-trinitrotoluene studied by corona discharge ion mobility-mass spectrometry. International Journal of Mass Spectrometry. **380**, 12-20 (2015)
134. Laakia, J., Pedersen, C.S., Adamov, A., Viidanoja, J., Syseov, A., Kotiaho, T.: Ion mobility spectrometry/ mass spectrometry (IMS/MS) for measurement of selected phenols, (Poster). IMSC 2009 (18th International Mass Spectrometry Conference, Bremen, Germany). (2009)
135. Robb, D.B., Blades, M.W.: Atmospheric Pressure Photoionization for Ionization of Both Polar and Nonpolar Compounds in Reversed-Phase LC/MS. Analytical Chemistry. **78**, 8162-8164 (2006)
136. Syage, J.A.: Mechanism of $[M + H]^+$ formation in photoionization mass spectrometry. Journal of the American Society for Mass Spectrometry. **15**, 1521-1533 (2004)
137. Karpas, Z., Berant, Z., Stimac, R.: An ion mobility spectrometry/mass spectrometry (IMS/MS) study of the site of protonation in anilines. Structural Chemistry. **1**, 201-204 (1990)
138. Karpas, Z.: Ion Mobility Spectrometry of Aliphatic and Aromatic Amines. Analytical Chemistry. **61**, 684-689 (1989)
139. Karpas, Z., Berant, Z.: Effect of drift gas on mobility of ions. The Journal of Physical Chemistry. **93**, 3021-3025 (1989)
140. Karasek, F.W., Kim, S.H., Rokushika, S.: Plasma chromatography of alkyl amines. Analytical Chemistry. **50**, 2013-2016 (1978)

141. Karpas, Z., Bell, S.E., Wang, Y.F., Walsh, M., Eiceman, G.A.: The structure of protonated diamines and polyamines. Structural Chemistry. **5**, 135-140 (1994)
142. Asbury, G.R., Hill, H.H.: Using Different Drift Gases To Change Separation Factors (α) in Ion Mobility Spectrometry. Analytical Chemistry. **72**, 580-584 (1999)
143. Matz, L.M., Hill Jr, H.H., Beegle, L.W., Kanik, I.: Investigation of drift gas selectivity in high resolution ion mobility spectrometry with mass spectrometry detection. Journal of the American Society for Mass Spectrometry. **13**, 300-307 (2002)
144. Figueiredo, A.M.F., Braga, J.A.E., Zabalaga, J.C., Oliveira, J.J., Aguiar, G.A., Silva, O.B., Mato, L.F., Daniel, L.M.F., Magnavita, L.P., Bruhn, C.H.L., .: Recôncavo Basin, Brazil: a prolific intracontinental rift basin. In: Landon, S.M. (Ed.), Interior rift basins. Memoir, 59. American Association of Petroleum Geologists, Tulsa. (1994)
145. Santos, C.F., Braga, J.A.E.: O estado da arte da Bacia do Recôncavo. Boletim de Geociências da Petrobras. **4**, (1990)
146. Coutinho, L.F.C.: Análise do Balanço Material do Petróleo em uma Região em Fase de Exploração Matura – Bacia Do Recôncavo, Brasil. PEC-COPPE/UFRJ. Thesis. (2008)
147. Nytoft, H.P., Lutnæs, B.F., Johansen, J.E.: 28-Nor-spergulanes, a novel series of rearranged hopanes. Organic Geochemistry. **37**, 772-786 (2006)
148. Eigenbrode, J.L., Freeman, K.H., Summons, R.E.: Methylhopane biomarker hydrocarbons in Hamersley Province sediments provide evidence for Neoarchean aerobiosis. Earth and Planetary Science Letters. **273**, 323-331 (2008)
149. Welander, P.V., Summons, R.E.: Discovery, taxonomic distribution, and phenotypic characterization of a gene required for 3-methylhopanoid production. Proceedings of the National Academy of Sciences. **109**, 12905-12910 (2012)
150. Chen, B., Liang, C., Yang, J., Contreras, D.S., Clancy, Y.L., Lobkovsky, E.B., Yaghi, O.M., Dai, S.: A Microporous Metal–Organic Framework for Gas-Chromatographic Separation of Alkanes. Angewandte Chemie. **118**, 1418-1421 (2006)
151. Trendel, J.-M., Restle, A., Connan, J., Albrecht, P.: Identification of a novel series of tetracyclic terpene hydrocarbons (C_{24}-C_{27}) in sediments and petroleums. Journal of the Chemical Society, Chemical Communications. 304-306 (1982)
152. May, J.C., McLean, J.A.: Advanced Multidimensional Separations in Mass Spectrometry: Navigating the Big Data Deluge. Annual Review of Analytical Chemistry. **9**, 387-409 (2016)